

## MULTI-COLOR AND TESS PHOTOMETRIC INVESTIGATION OF FOUR LOW MASS-RATIO CONTACT BINARY SYSTEMS

AHMED WAQAS ZUBAIRI,<sup>1,2</sup> ZHAO ERGANG,<sup>1,3,4</sup> QIAN SHENGBANG,<sup>5</sup> ZHOU XIAO,<sup>1,3,4</sup> AND EDUARDO FERNÁNDEZ LAJÚS<sup>6,7</sup>

<sup>1</sup> Yunnan Observatories, Chinese Academy of Sciences (CAS), , 650216 Kunming, China

<sup>2</sup> University of Chinese Academy of Sciences, No.1 Yanqihe East Rd, Huairou District, Beijing, PR China, 101408

<sup>3</sup> Center for Astronomical Mega-Science, Chinese Academy of Sciences, 20A Datun Road, Chaoyang District, Beijing, 100012, P. R. China

<sup>4</sup> Key Laboratory of the Structure and Evolution of Celestial Objects, Chinese Academy of Sciences, P. O. Box 110, 650216 Kunming, China

<sup>5</sup> Department of Astronomy, Yunnan University, Kunming 650091, P. R. China

<sup>6</sup> Facultad de Ciencias Astronómicas y Geofísicas, Universidad Nacional de La Plata, Paseo del Bosques/n, 1900 La Plata, Buenos Aires, Argentina

<sup>7</sup> Instituto de Astrofísica de La Plata (CCT La Plata – CONICET/UNLP), 1900 La Plata, Argentina

### ABSTRACT

We present the TESS and  $BVR_cI_c$  light curves solution of four low mass-ratio contact binary systems TIC 159102550, V1068 Her, MW Pav and TIC 321576458. Except MW Pav, all three systems have been studied for the first time. The  $BVR_cI_c$  observations of southern contact binary system, MW Pav, is carried out using 60cm Helen Sawyer Hogg (HSH) telescope located at Argentina. The TIC 321576458 is observed in  $BVR_cI_c$  with 70cm Sino-Thai telescope at Lijiang station of Yunnan Observatories. The period analysis of TIC 159102550 show anti-correlation between primary and secondary minima and no long term variation is reported. The systems V1068 Her and MW Pav show increasing period at  $dP/dt = 1.247(9) \times 10^{-7} \text{days/yr}$  and  $dP/dt = 2.256(6) \times 10^{-7} \text{days/yr}$ , respectively. Data for TIC 321576458 is too few to determine any periodic variations. The light curve analysis using Wilson-Dominney model shows that systems are low mass-ratio contact binaries. Out of four targets, two systems TIC 159102550 and V1068 Her, are shallow contact binary systems with fill-out factor of 20% and 14%, respectively. The two contact binaries MW Pav and TIC 321576458 are in deep contact state with fill-out factor 63% and 61%, respectively. V1068 Her shows EB-type light curve, however the temperature difference between the primary secondary component is only 17K, which indicates that system is in thermal contact. To understand the evolutionary status of these systems, the components are plotted on the mass-luminosity diagram. The primary companions are in the ZAMS zone while the secondary components of all the systems are away from TAMS which indicates that secondary is more evolved than the primary components. V1068 Her and MW Pav are expected to evolve into a single rapidly rotating star provided that they meet the well-known Hut's criterion. Through statistical investigation of more than hundred low mass-ratio contact binary systems including our targets, we have found that all of the low mass-ratio contact binaries have undergone the mass-ratio inversion process. Based on our sample, the relationship between mass ratio and spin and orbital angular momentum ratio has been updated and proposed a new value of  $q_{min} = 0.0388$  for Darwin's stability.

*Keywords:* binaries: eclipsing; —binaries: close; — stars: evolution; —stars: individual: TIC 159102550, V1068 Her, MW Pav & TIC 321576458

### 1. INTRODUCTION

The two Roche lobe filled components of an eclipsing binary star formed a common convective envelope are referred as W UMa type eclipsing binary systems or simply contact binaries (Kopal 1956; Lucy 1968). These binaries are further divided into two categories; A-type and W-type (Binnendijk 1970; Lucy 1968). The continuous variation in the light curve along with small difference between primary and secondary minima put them in EW-type eclipsing binary

system. The small difference (nearly equal) depths in both minima indicates that the temperature of primary and secondary star is almost equal. However, the variation in magnitude at maxima shows the magnetic activity which can be explained with the presence of star spots (O'Connell 1951). The orbital period study of contact binaries is also important. The orbital and spin angular momentum plays an important role in maintaining orbital stability (Hut 1980; Counselman 1973) and provide useful information about the rate of mass transfer and angular momentum loss and help us to identify the potential merger candidates (e.g., Ferreira et al. (2019)).

The widely accepted point of view about the formation of these system is via evolution from detached binaries due to AML or Kozai cycle. The strong interaction of binary companions makes their evolutionary scenario totally different compared to single star evolution. Some marginal contact systems are believed to be newly-formed contact binaries and are at the beginning of their contact phase (Qian et al. 2017; Qian et al. 2018, 2020). Their evolutionary process can be explained by the combination of angular momentum loss (AML) and thermal relaxation oscillation (TRO). Such system oscillate around a critical mass-ratio (Lucy 1976; Flannery 1976; Robertson & Eggleton 1977; Qian 2001, 2003; Zhu et al. 2014). These systems are expected to merge sooner into FK Comae type or blue straggler stars (Qian et al. 2005b, 2008; Zhu et al. 2014; Sriram et al. 2016; Zhu et al. 2016; Gao et al. 2022). Therefore, contact binaries, especially with low mass-ratio, work as natural laboratories for studying the mass and energy transfer, the angular momentum loss of the system, and stellar evolution & merging processes.

In this paper, we are presenting photometric investigation of four low mass-ratio contact binary systems. As a time of this writing, three systems (TIC 159102550, V1068 Her and TIC 321576458) have not been studied in detailed before. We are presenting the first photometric investigation for these systems. The MW Pav(MW Pavonis) is a low-mass ratio contact binary system in southern hemisphere. The first photometric solution was presented by Eggen (1968). Later on, Williamon (1971) and Lapasset (1977) also observed MW Pav but did not present any detailed solution. The radial velocity solution of Rucinski & Duerbeck (2006) reported the spectral type to be F3/IV-V along with spectroscopic mass ratio of  $q_{sp} = 0.228$  which was not consistent with their photometric mass-ratio ( $q_{ph} = 0.122$ ). Deb & Singh (2011), uses the spectroscopic mass-ratio of Rucinski & Duerbeck (2006) and face problems in light curve fitting. However, they proposed the photometric mass-ratio of  $q = 0.200$  with 52% degree of contact. More recently, Alvarez et al. (2015), presented combined light and velocity curve solution. Their UBV photometric solution suggest a new mass-ratio  $q = 0.222$  and a high fill-out factor of 60% for the system.

## 2. OBSERVATIONS

### 2.1. *TESS Observations*

The Transiting Exoplanet Survey Satellite (TESS) has rapidly increased the eclipsing binaries research (Ricker et al. 2014). The obtained photometric data of a number of eclipsing binaries can be downloaded from Mikulski Archive for Space Telescopes (MAST) archive.<sup>1</sup>

The TIC 159102550 ( $\alpha_{2000} = 19^h 18^m 17.44^s$ ,  $\delta_{2000} = +42^\circ 02' 47.39''$ ) is listed as EW type binary in VSX catalog. The system is observed by TESS from May 14, 2020 to June 08, 2020 in sector 25 and 26 respectively. The data of V1068 Her (=TIC 193580427) ( $\alpha_{2000} = 17^h 43^m 23.08^s$ ,  $\delta_{2000} = +47^\circ 51' 41.79''$ ) is available from July 24, 2021 to August 20, 2021 in sector 41.

Both of these two targets (TIC 159102550 and V1068 Her) were also observed by LAMOST (Wu et al. 2011; Cui et al. 2012). The obtained atmospheric parameters are listed in Table 1.

**Table 1.** Atmospheric parameter of TIC 159102550 and V1068 Her observed by LAMOST

Target	UT date	Spectral Class	$T_{eff}(K)$	$\log(g)(cm/s^2)$	[Fe/H](dex)
V1068 Her	18 May 2016	F5	$6605.09 \pm 12.23$	$4.197 \pm 0.019$	$0.04 \pm 0.01$
TIC 159102550	08 March 2015	G0	$6158.85 \pm 50.28$	$4.168 \pm 0.083$	$0.21 \pm 0.04$

### 2.2. *BVR<sub>c</sub>I<sub>c</sub> Observations*

MW Pav (=TIC 372127422) ( $\alpha_{2000} = 20^h 46^m 27.74^s$ ,  $\delta_{2000} = -71^\circ 56' 58.46''$ ,  $V_{mag} = 8.79$ ) has been observed with 60cm Helen Sawyer Hogg (HSH) telescope at Complejo Astronomico El Leoncito (CASLEO), San Juan, Argentina.

<sup>1</sup> <https://mast.stsci.edu/portal/Mashup/Clients/Mast/Portal.html>

The new multi-color light curve is taken during three nights on August 09, 15, 20, 2019. These observations were carried out using SBIG STL1001E CCD camera with standard Jhonson's  $BVR_cI_c$  filters attached to the HSH telescope giving  $9.3' \times 9.3'$  field of view. MW Pavis also observed by TESS from July 05, 2020 to September 30, 2020 in sector-27 using 2-minutes cadence. The differential magnitudes from HSH observations are determined using the standard aperture photometry procedure in Image Reduction and Data Analysis Facility (IRAF) software packages (Tody 1986, 1993).

TIC 321576458 ( $\alpha_{2000} = 15^h 42^m 12.72^s$ ,  $\delta_{2000} = +37^\circ 52' 46.50''$ ,  $V_{mag} = 13.74$ ) has been observed with 70cm Sino-Thai telescope at Lijiang station of Yunnan Observatories. The first  $BVR_cI_c$  light curve of TIC 321576458 is obtained on April 13 and April 17, 2023. The telescope is equipped with Andor iKon 936 (2048x2048) CCD camera with standard Jhonson's  $BVR_cI_c$  filters. The system is also observed by TESS from July 05, 2020 to September 30, 2020 in sector-27 using 2-minutes cadence. The differential magnitudes from the observations of 70cm Sino-Tahi telescope are determined using the standard aperture photometry procedure in Image Reduction and Data Analysis Facility (IRAF) software packages (Tody 1986, 1993).

### 3. ORBITAL PERIOD INVESTIGATION

#### 3.1. Period Study of TIC 159102550

The period search of TIC 159102550 gives  $0.488253d$  from ROTSE All-Sky Surveys (Akerlof et al. 2000). No other database has any information on previously published period of TIC 159102550. Therefore, the O-C values are determined by using epoch  $MinI = BJD2459446.1702 + 0.488253E$ .

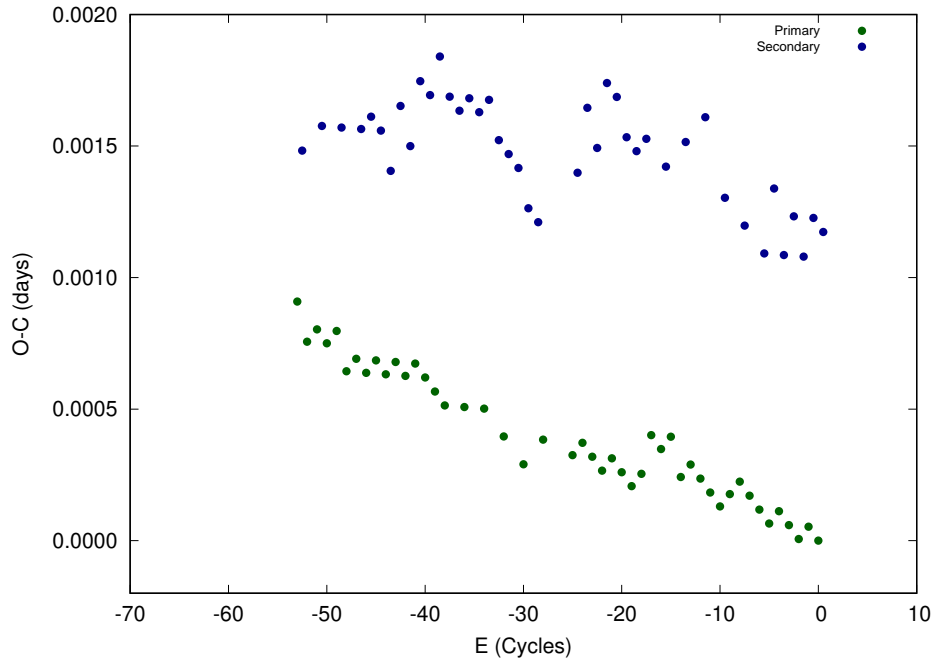


**Figure 1.** O-C diagram of TIC 159102550. The primary and secondary minimas shows anti-correlation.

The Figure 1 shows that primary and secondary minimas are anti-correlated with each other. It further indicates that the period should be corrected from left upper panel of Figure 2 for the primary minima. The revised ephemeris and period are given in Equation 1. A sample of times of primary and secondary minima are listed in Table 3.1.

$$MinI = BJD2459446.1702(7) + 0.48823883(8) \times E \quad (1)$$

We reconstruct the O-C diagram with the corrected period and ephemeris which is displayed in right panel of Figure 2. The O-C for primary minima does not displays any large-scale variation as shown in upper panel of Figure 2, which means that the revised period gives a better value than before. However, the corrected period from secondary minima

shows a different behavior as shown in below panel of Figure 2. The revised O-C values are also tabulated in Table 3.1.

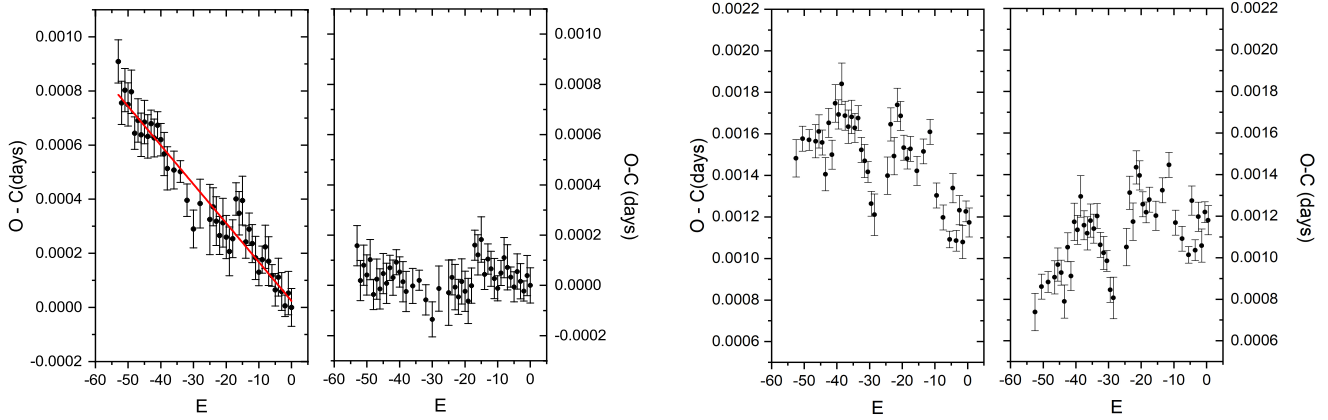


**Figure 2.** O-C diagram of TIC 159102550. Left panel is calculated by the original period for the primary minima and display the revised one. The right panel is the same but for secondary minima.

**Table 2.** Times of minima for TIC 159102550. The BJD are +2400000.

BJD	Error	Type	Method	E(Cycles)	$(O - C)_1$	$(O - C)_2$	Reference
59420.29370	0.00008	p	TESS	-53.00	0.00091	0.00016	Present study
59420.78180	0.00008	p	TESS	-52.00	0.00076	0.00002	Present study
59420.78180	0.00008	p	TESS	-52.00	0.00076	0.00002	Present study
59421.27010	0.00008	p	TESS	-51.00	0.00080	0.00008	Present study
.....	.....	.	....	....	.....	.....	.....
59444.21730	0.00007	p	TESS	-4.00	0.00011	0.00006	Present study
59444.70550	0.00007	p	TESS	-3.00	0.00006	0.00002	Present study
59445.19370	0.00004	p	TESS	-2.00	0.00001	-0.00002	Present study
59445.68200	0.00008	p	TESS	-1.00	0.00005	0.00004	Present study
.....	.....	.	....	....	.....	.....	.....
59420.53840	0.00009	s	TESS	-52.50	0.00148	0.00074	Present study
59421.51500	0.00006	s	TESS	-50.50	0.00158	0.00086	Present study
59422.49150	0.00005	s	TESS	-48.50	0.00157	0.00088	Present study
59423.46800	0.00008	s	TESS	-46.50	0.00156	0.00091	Present study
.....	.....	.	....	....	.....	.....	.....
59444.46240	0.00005	s	TESS	-3.50	0.00109	0.00104	Present study
59444.95080	0.00007	s	TESS	-2.50	0.00123	0.00120	Present study
59445.43890	0.00008	s	TESS	-1.50	0.00108	0.00106	Present study
59445.92730	0.00005	s	TESS	-0.50	0.00123	0.00122	Present study
.....	.....	.	....	....	.....	.....	.....

### 3.2. Long term Period variation of V1068 Her

The newly determined times of minima of V1068 Her along with values available in literature are listed in Table 3. All HJDs are converted to BJD using <https://astroutils.astronomy.osu.edu/time/hjd2bjd.html>. The new O-C values are calculated by using the following epoch  $MinI = BJD245934.9772 + 0.394304E$ . The trend of O-C values indicate an upward parabolic fit, as shown in the Figure 3. The least square method yields that period of V1068 Her is increasing. We obtained the new ephemeris and period of V1068 Her as shown in Equation 2.

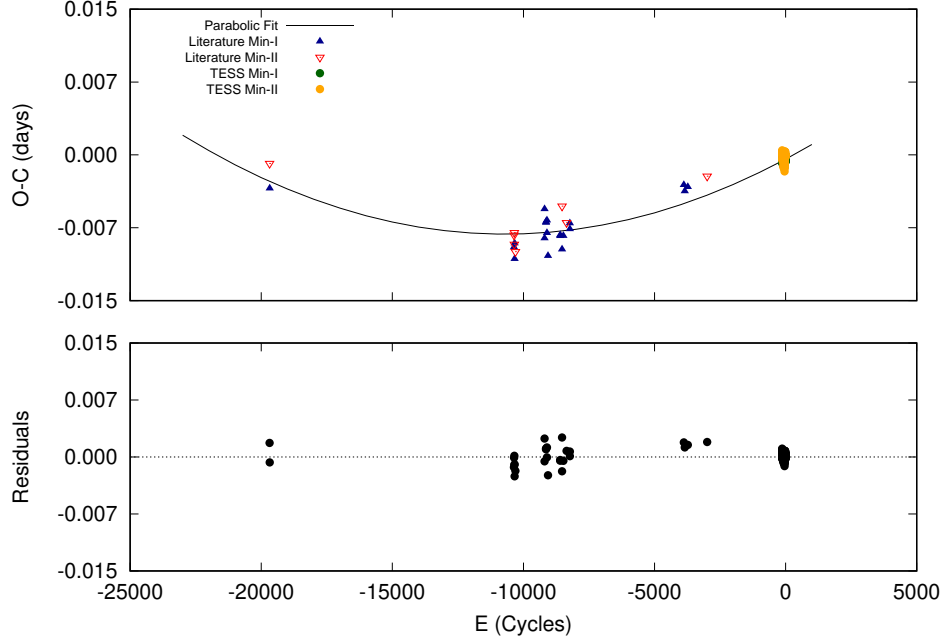


**Figure 3.** O-C diagram of V1068 Her with all available times of minima. The parabolic fit is shown in black line. Residuals are plotted in the bottom panel.

$$MinI = 2459034.9767(6) + 0.39430544(2) \times E + 6.73(5) \times 10^{-11} E^2 \quad (2)$$

The quadratic term in Equation 2 leads us to determine the period increase at rate of  $dP/dt = 1.247(9) \times 10^{-7} \text{ days/yr}$ .

**Table 3.** Times of minima for V1068 Her. The BJD are +2400000

BJD	Error	Type	Method	E(Cycles)	O-C(days)	Reference
51274.87645	-	s	ccd	-19680.50	-0.000881	Diethelm (2001)
51275.85965	-	p	ccd	-19678.00	-0.003441	Diethelm (2001)
54950.37256	-	p	R	-10359.00	-0.009505	Brat et al. (2009)
54950.57096	-	s	R	-10358.50	-0.008257	Brat et al. (2009)
54954.51306	-	s	I	-10348.50	-0.009197	Brat et al. (2009)
54954.51426	-	s	R	-10348.50	-0.007997	Brat et al. (2009)
54959.44036	-	p	I	-10336.00	-0.010697	Brat et al. (2011)
54959.44196	-	p	R	-10336.00	-0.009097	Brat et al. (2011)
54971.46736	-	s	-Ir	-10305.50	-0.009969	Hubscher et al. (2010)
55410.52626	-	p	I	-9192.00	-0.008568	Brat et al. (2011)
55410.52926	-	p	R	-9192.00	-0.005568	Brat et al. (2011)
55431.42596	-	p	V	-9139.00	-0.006980	Brat et al. (2011)
55431.42606	-	p	B	-9139.00	-0.006880	Brat et al. (2011)
55446.40846	-	p	I	-9101.00	-0.008031	Brat et al. (2011)

**Table 3.** Times of minima for V1068 Her. The BJD are +2400000

BJD	Error	Type	Method	E(Cycles)	O-C(days)	Reference
55446.40977	-	p	R	-9101.00	-0.006731	Brat et al. (2011)
55461.38967	-	p	-Ir	-9063.00	-0.010383	Hubscher et al. (2012)
55645.53167	-	p	I	-8596.00	-0.008349	Hoňková et al. (2013)
55645.53177	-	p	R	-8596.00	-0.008249	Hoňková et al. (2013)
55672.34297	-	p	-Ir	-8528.00	-0.009721	Hubscher et al. (2012)
55672.54457	-	s	-Ir	-8527.50	-0.005273	Hubscher et al. (2012)
55692.45387	-	p	-Ir	-8477.00	-0.008324	Hubscher et al. (2012)
55741.54607	-	s	-Ir	-8352.50	-0.006972	Hubscher et al. (2012)
55791.42487	-	p	I	-8226.00	-0.007628	Hoňková et al. (2013)
55791.42547	-	p	R	-8226.00	-0.007028	Hoňková et al. (2013)
57504.68028	-	p	-I-U	-3881.00	-0.003093	Pagel (2020)
57518.48028	-	p	-I	-3846.00	-0.003733	Hubscher (2017)
57563.43138	-	p	-I-U	-3732.00	-0.003290	Pagel (2020)
57854.62599	-	s	-I-U	-2993.50	-0.002185	Pagel (2020)
58983.71710	0.00011	p	TESS	-130.00	-0.000580	Present study
58984.11170	0.00009	p	TESS	-129.00	-0.000284	Present study
58984.50590	0.00008	p	TESS	-128.00	-0.000388	Present study
58984.90020	0.00007	p	TESS	-127.00	-0.000392	Present study
.....	.....	.	....	.....	.....	.....
59033.39960	0.00009	p	TESS	-4.00	-0.000384	Present study
59033.79390	0.00007	p	TESS	-3.00	-0.000388	Present study
59034.18820	0.00008	p	TESS	-2.00	-0.000392	Present study
59034.58260	0.00008	p	TESS	-1.00	-0.000296	Present study
59034.97720	0.00008	p	TESS	0.00	0.000000	Present study
.....	.....	.	....	.....	.....	.....
58983.91530	0.00012	s	TESS	-129.50	0.000468	Present study
58984.30950	0.00008	s	TESS	-128.50	0.000364	Present study
58984.70370	0.00012	s	TESS	-127.50	0.000260	Present study
58985.49230	0.00011	s	TESS	-125.50	0.000252	Present study
58985.88650	0.00012	s	TESS	-124.50	0.000148	Present study
.....	.....	.	....	.....	.....	.....
59032.80840	0.00009	s	TESS	-5.50	-0.000128	Present study
59033.20260	0.00009	s	TESS	-4.50	-0.000232	Present study
59033.59710	0.00008	s	TESS	-3.50	-0.000036	Present study
59034.38570	0.00007	s	TESS	-1.50	-0.000044	Present study
59034.78000	0.00008	s	TESS	-0.50	-0.000048	Present study
.....	.....	.	....	.....	.....	.....

### 3.3. Long term Period variation of MW Pav

The first observations were presented by Eggen (1968) with a period of 0.562979 days. Later on, the different period of MW Pav, was reported by many authors (Williamon 1971; Lapasset 1977). The radial velocity solution of Rucinski & Duerbeck (2006) suggests that the period of system is 0.7949810days. The O-C gateway<sup>2</sup> and the spreadsheets of Bob Nelson, maintained at AAVSO database (Bob 2011) contains most of the data which we have used during period investigation. Table 4 contains all the values that have been collected from the literature,  $BVR_cI_c$  filters at HSH telescope and TESS data. All HJDs are converted into BJD. The O-C diagram indicates parabolic fit

<sup>2</sup> <http://var2.astro.cz/ocgate>

as shown in the Figure 4. The least-square method was applied to obtain new ephemeris and period of MW Pav as shown in Equation 3.

$$MinI = 2458704.61313(8) + 0.79499753(5) \times E + 2.417(3) \times 10^{-10} E^2 \quad (3)$$

The quadratic term in Equation 3 helped us to determine the period increase rate of  $dP/dt = 2.220(9) \times 10^{-7} \text{ days/yr}$ . If we compare this value with Alvarez et al. (2015), it can be noted that the rate of increase in period has been boosted up by  $2.213 \times 10^{-7} \text{ days/yr}$ .

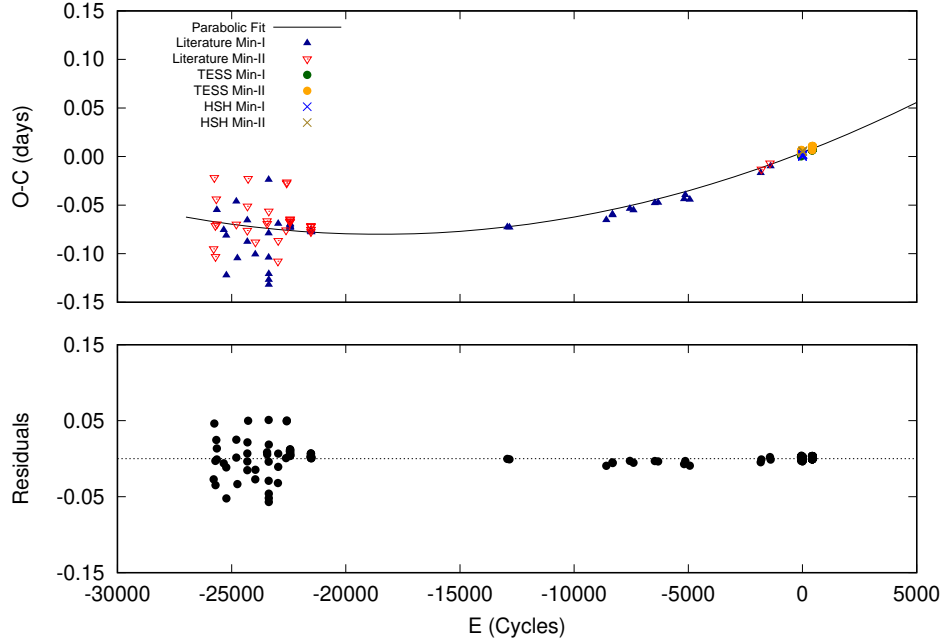


**Figure 4.** The O-C diagram of MW Pav is constructed using  $MinI = HJD2458704.6089 + 0.79498855E$ . Black line shows parabolic fit. Residuals are plotted in the bottom panel.

**Table 4.** Times of minima for MW Pav. The BJD are +2400000

BJD	Error	Type	Method	E(Cycles)	O-C(days)	Reference
38204.5424	-	s	pg	-25786.5	-0.0950	Eggen (1968)
38228.4654	-	s	pg	-25756.5	-0.0217	Eggen (1968)
38263.3954	-	s	pg	-25712.5	-0.0711	Eggen (1968)
38267.3384	-	s	pg	-25707.5	-0.1031	Eggen (1968)
38295.2224	-	s	pg	-25672.5	-0.0437	Eggen (1968)
38314.2764	-	s	pg	-25648.5	-0.0694	Eggen (1968)
38316.2784	-	p	pg	-25646.0	-0.0549	Eggen (1968)
38555.5494	-	p	pg	-25345.0	-0.0754	Eggen (1968)
38641.4024	-	p	pg	-25237.0	-0.0812	Eggen (1968)
38649.3114	-	p	pg	-25227.0	-0.1221	Eggen (1968)
38992.4014	-	s	pg	-24795.5	-0.0696	Eggen (1968)
38994.4124	-	p	pg	-24793.0	-0.0461	Eggen (1968)
39029.3334	-	p	pg	-24749.0	-0.1046	Eggen (1968)
39374.3754	-	p	pg	-24315.0	-0.0876	Eggen (1968)
39376.3744	-	s	pg	-24312.5	-0.0761	Eggen (1968)
39378.3724	-	p	pg	-24310.0	-0.0655	Eggen (1968)

**Table 4.** Times of minima for MW Pav. The BJD are +2400000

BJD	Error	Type	Method	E(Cycles)	O-C(days)	Reference
39380.3744	-	s	pg	-24307.5	-0.0510	Eggen (1968)
39404.2524	-	s	pg	-24277.5	-0.0227	Eggen (1968)
39654.1985	-	p	pg	-23963.0	-0.1006	Eggen (1968)
39656.1985	-	s	pg	-23960.5	-0.0880	Eggen (1968)
40064.0495	-	s	pg	-23447.5	-0.0661	Lapasset (1974)
40068.0215	-	s	pg	-23442.5	-0.0691	Lapasset (1974)
40120.0585	-	p	pg	-23377.0	-0.1038	Eggen (1968)
40120.0835	-	p	pg	-23377.0	-0.0788	Eggen (1968)
40120.9335	-	p	pg	-23376.0	-0.0238	Eggen (1968)
40122.8885	-	s	pg	-23373.5	-0.0563	Eggen (1968)
40124.0055	-	p	pg	-23372.0	-0.1318	Eggen (1968)
40124.0105	-	p	pg	-23372.0	-0.1268	Eggen (1968)
40124.0165	-	p	pg	-23372.0	-0.1208	Eggen (1968)
40440.0375	-	s	pg	-22974.5	-0.1077	Lapasset (1974)
40450.0135	-	p	pg	-22962.0	-0.0691	Lapasset (1974)
40451.9835	-	s	pg	-22959.5	-0.0866	Lapasset (1974)
40722.2905	-	s	pg	-22619.5	-0.0757	Lapasset (1974)
40746.1885	-	s	pg	-22589.5	-0.0273	Lapasset (1974)
40750.1645	-	s	pg	-22584.5	-0.0263	Lapasset (1974)
40862.6085	-	p	B	-22443.0	-0.07318	Williamon (1971)
40862.6105	-	p	V	-22443.0	-0.07118	Williamon (1971)
40862.6116	-	p	U	-22443.0	-0.07008	Williamon (1971)
40863.8070	-	s	B	-22441.5	-0.06716	Williamon (1971)
40863.8070	-	s	U	-22441.5	-0.06716	Williamon (1971)
40863.8089	-	s	V	-22441.5	-0.06526	Williamon (1971)
40864.6020	-	s	V	-22440.5	-0.06715	Williamon (1971)
40864.6040	-	s	U	-22440.5	-0.06515	Williamon (1971)
40864.6048	-	s	B	-22440.5	-0.06435	Williamon (1971)
40870.5589	-	p	B	-22433.0	-0.07266	Williamon (1971)
40870.5590	-	p	U	-22433.0	-0.07256	Williamon (1971)
40870.5620	-	p	V	-22433.0	-0.06956	Williamon (1971)
41587.6340	-	p	U	-21531.0	-0.07722	Lapasset (1974)
41587.6352	-	p	B	-21531.0	-0.07602	Lapasset (1974)
41587.6357	-	p	V	-21531.0	-0.07552	Lapasset (1974)
41589.6266	-	s	U	-21528.5	-0.07209	Lapasset (1974)
41589.6270	-	s	B	-21528.5	-0.07169	Lapasset (1974)
41589.6275	-	s	V	-21528.5	-0.07119	Lapasset (1974)
41592.8012	-	s	U	-21524.5	-0.07744	Lapasset (1974)
41592.8036	-	s	V	-21524.5	-0.07504	Lapasset (1974)
41592.8036	-	s	B	-21524.5	-0.07504	Lapasset (1974)
41606.7131	-	p	U	-21507.0	-0.07784	Lapasset (1974)
41606.7137	-	p	B	-21507.0	-0.07724	Lapasset (1974)
41606.7149	-	p	V	-21507.0	-0.07604	Lapasset (1974)
48426.1301	0.0026	p	V	-12929.0	-0.07264	Esa (1997)
48500.0637	-	p	V	-12836.0	-0.07297	Esa (1997)
51874.7978	-	p	V	-8591.0	-0.06529	Pojmanski (2002)
52085.4756	0.0020	p	V	-8326.0	-0.05945	Pojmanski (2002)
52096.6047	0.0033	p	V	-8312.0	-0.06019	Pojmanski (2002)

**Table 4.** Times of minima for MW Pav. The BJD are +2400000

BJD	Error	Type	Method	E(Cycles)	O-C(days)	Reference
52694.4426	0.0017	p	V	-7560.0	-0.05367	Pojmanski (2002)
52820.8443	0.0021	p	V	-7401.0	-0.05515	Pojmanski (2002)
53564.9609	0.0023	p	V	-6465.0	-0.04775	Pojmanski (2002)
53679.4396	0.0017	p	V	-6321.0	-0.04741	Pojmanski (2002)
54584.9352	0.0018	p	V	-5182.0	-0.04377	Pojmanski (2002)
54626.2789	0.0021	p	V	-5130.0	-0.03947	Pojmanski (2002)
54782.8869	0.0021	p	V	-4933.0	-0.04422	Pojmanski (2002)
57248.1738	0.003	p	V	-1832.0	-0.01686	Richards et al. (2016)
57273.2198	0.003	s	V	-1800.5	-0.01300	Richards et al. (2016)
57572.1418	0.004	s	V	-1424.5	-0.00670	Richards et al. (2017)
57593.2058	0.004	p	V	-1398.0	-0.00989	Richards et al. (2017)
58704.6097	0.0002	p	B	0.0	0.00000	Present study
58704.6097	0.0002	p	V	0.0	0.00000	Present study
58704.6108	0.0002	p	R	0.0	0.00110	Present study
58704.6116	0.0002	p	I	0.0	0.00190	Present study
58710.5781	0.0002	s	B	7.5	0.00600	Present study
58710.5779	0.0002	s	V	7.5	0.00582	Present study
58710.5775	0.0002	s	R	7.5	0.00539	Present study
58710.5770	0.0002	s	I	7.5	0.00493	Present study
58715.7412	0.0002	p	B	14.0	0.00166	Present study
58715.7421	0.0002	p	V	14.0	0.00256	Present study
58715.7414	0.0002	p	R	14.0	0.00186	Present study
58715.7413	0.0002	p	I	14.0	0.00176	Present study
58654.5281	0.0021	P	TESS	-63.0	0.00271	Present study
58656.1180	0.0011	P	TESS	-61.0	0.00263	Present study
58656.9098	0.0014	P	TESS	-60.0	-0.00056	Present study
58660.0929	0.0004	P	TESS	-56.0	0.00259	Present study
.....	.....	.	.	.....	.....	.....
58662.4769	0.0008	P	TESS	-53.0	0.00162	Present study
58663.2721	0.0007	P	TESS	-52.0	0.00183	Present study
58665.6567	0.0007	P	TESS	-49.0	0.00147	Present study
58666.4518	0.0006	P	TESS	-48.0	0.00158	Present study
.....	.....	.	.	.....	.....	.....
58654.1322	0.0006	S	TESS	-63.5	0.00429	Present study
58656.5174	0.0016	S	TESS	-60.5	0.00453	Present study
58658.9027	0.0008	S	TESS	-57.5	0.00489	Present study
58659.6979	0.0002	S	TESS	-56.5	0.00510	Present study
.....	.....	.	.	.....	.....	.....
58660.4927	0.0016	S	TESS	-55.5	0.00489	Present study
58662.0824	0.0020	S	TESS	-53.5	0.00465	Present study
58662.8780	0.0005	S	TESS	-52.5	0.00528	Present study
58663.6730	0.0004	S	TESS	-51.5	0.00528	Present study
.....	.....	.	.	.....	.....	.....

### 3.4. Period Study of TIC 321576458

The period of TIC 321576458 was first reported to be 0.37614d by (Drake et al. 2014). No times of minimas are available for this target as of this writing. We have determine new times of primary and secondary minima from our

$BVR_cI_c$  observations and TESS light curves using Kwee & Wan Woerden algorithm (Kwee & van Woerden 1956). The O-C diagram is shown in Figure 5 and the times of primary and secondary minima are tabulated in Table 5. The figure clearly shows no variation in the orbital period. The new period and ephemeris are shown in Equation 4.

$$\text{MinI} = 2460052.3995(2) + 0.376144829(1) \times E \quad (4)$$

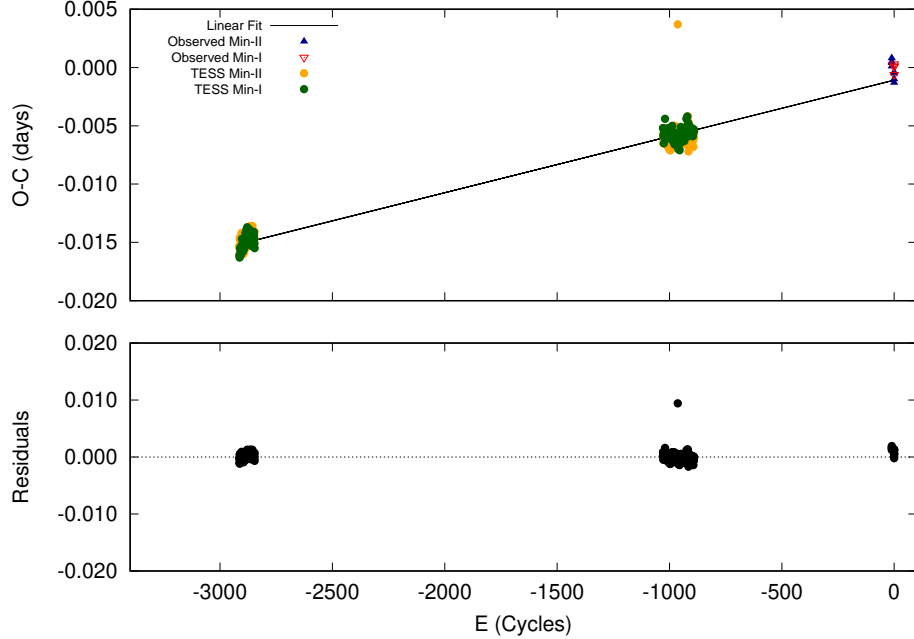


**Figure 5.** The O-C diagram of TIC 321576458 is constructed using  $\text{MinI} = BJD2460052.39813 + 0.37614E$ . Residuals are plotted in the bottom panel.

**Table 5.** A sample of Times of minima for TIC 321576458. The BJD are +2400000

BJD	Error	Type	Method	E(Cycles)	O-C(days)	Reference
60052.39723	0.00034	P	B	0.0	-0.000903	Present study
60052.39793	0.00023	P	Ic	0.0	-0.000203	Present study
60052.39793	0.00020	P	Rc	0.0	-0.000203	Present study
60052.39813	0.00019	P	V	0.0	-0.000003	Present study
58956.30971	0.00049	P	TESS	-2914.0	-0.016460	Present study
58956.68565	0.00064	P	TESS	-2913.0	-0.016660	Present study
58957.06191	0.00311	P	TESS	-2912.0	-0.016540	Present study
58957.43875	0.00115	P	TESS	-2911.0	-0.015840	Present study
58957.81440	0.00109	P	TESS	-2910.0	-0.016330	Present study
.....	.....	.	....	.....	.....	.....
59715.74690	0.00016	P	TESS	-895.0	-0.005930	Present study
59716.12320	0.00023	P	TESS	-894.0	-0.005770	Present study
59716.49920	0.00015	P	TESS	-893.0	-0.005910	Present study
59716.87560	0.00026	P	TESS	-892.0	-0.005650	Present study
59717.25170	0.00027	P	TESS	-891.0	-0.005690	Present study
.....	.....	.	....	.....	.....	.....
60048.26083	0.00023	S	B	-11.0	0.000236	Present study

**Table 5.** A sample of Times of minima for TIC 321576458. The BJD are +2400000

BJD	Error	Type	Method	E(Cycles)	O-C(days)	Reference
60052.20843	0.00024	S	B	-0.5	-0.001633	Present study
60052.20923	0.00026	S	$I_c$	-0.5	-0.000833	Present study
60048.26043	0.00046	S	$I_c$	-11.0	-0.000164	Present study
60048.26113	0.00019	S	$R_c$	-11.0	0.000536	Present study
60052.20933	0.00028	S	$R_c$	-0.5	-0.000733	Present study
60048.26073	0.00019	S	V	-11.0	0.000136	Present study
60052.20873	0.00017	S	V	-0.5	-0.001333	Present study
58956.12250	0.00051	S	TESS	-2914.5	-0.015600	Present study
58956.49840	0.00498	S	TESS	-2913.5	-0.015840	Present study
58956.87540	0.00253	S	TESS	-2912.5	-0.014980	Present study
58957.25160	0.00112	S	TESS	-2911.5	-0.014920	Present study
58957.62770	0.00158	S	TESS	-2910.5	-0.014960	Present study
.....	.....	.	....	.....	.....	.....
59715.93440	0.00023	S	TESS	-894.5	-0.006500	Present study
59716.30990	0.00033	S	TESS	-893.5	-0.007140	Present study
59716.68700	0.00022	S	TESS	-892.5	-0.006180	Present study
59717.06300	0.00016	S	TESS	-891.5	-0.006320	Present study
59717.43960	0.00020	S	TESS	-890.5	-0.005860	Present study

#### 4. LIGHT CURVE SOLUTIONS

We use Mode-3 of the Wilson-Divenney (WD) code to obtain the solution of light curves (Wilson & Devinney 1971; Wilson & Van Hamme 2014). According to Lucy (1967) and Ruciński (1969), the gravity darkening coefficients ( $g_1, g_2$ ) and albedos ( $A_1, A_2$ ) should be 0.32 and 0.5, respectively as these values are suitable for binaries with convective envelopes. The limb darkening parameters were obtained from van Hamme (1993). As per Mode-3 constraint in the WD program, the fixed parameters were  $g_1, g_2, A_1, A_2, x_1, x_2, y_1, y_2$ . The gravitational potentials are kept equal ( $\Omega_1 = \Omega_2$ ) for contact configuration.

##### 4.1. TIC 159102550

In the absence of spectroscopic and photometric mass-ratio of this target, we apply the well-known q-search process to estimate the mass-ratio of the system. According to Pribulla et al. (2003) a reliable mass-ratio can be obtained for totally eclipsing binary systems. The results showed in Figure 6 indicates  $q = 0.20$  for TIC 159102550.

We use this q-value and keep it adjustable along with  $T_2, \Omega_1, i, q$ , and  $L_1$  to get the final convergent solution. The temperature of primary component ( $T_1$ ) was opted from LAMOST data (Table 1). The modeled and observed data showed variation in amplitude of the light curve at phase 0.25 and 0.75. In order to cover this discrepancy in light curve solution, we introduced a cool spot on primary component for which parameters are listed in Table 8. The final light curve solution is shown in Figure 7.

The obtained photometric parameters are listed in Table 6

##### 4.2. V1068 Her

Since no photometric and spectroscopic mass ratio of this target was available in the literature, so we employed the q-search process to determine the unique value for the mass-ratio. The results of q-search method indicate the  $q = 0.28$  for V1068 Her. The results are displayed in Figure 6.

We use this q-value and keep it adjustable along with  $T_2, \Omega_1, i, q$ , and  $L_1$  to get the final convergent solution. The temperature of primary component ( $T_1$ ) was opted from Table 1. The convergent solution when superimposed on the observed data shows difference in Max-I and Max-II values. Therefore, we performed a spot solution on the light curve. The obtained photometric parameters are listed in Table 6 and the spot parameters are tabulated in Table 8. The final light curve solution is shown in Figure 7.

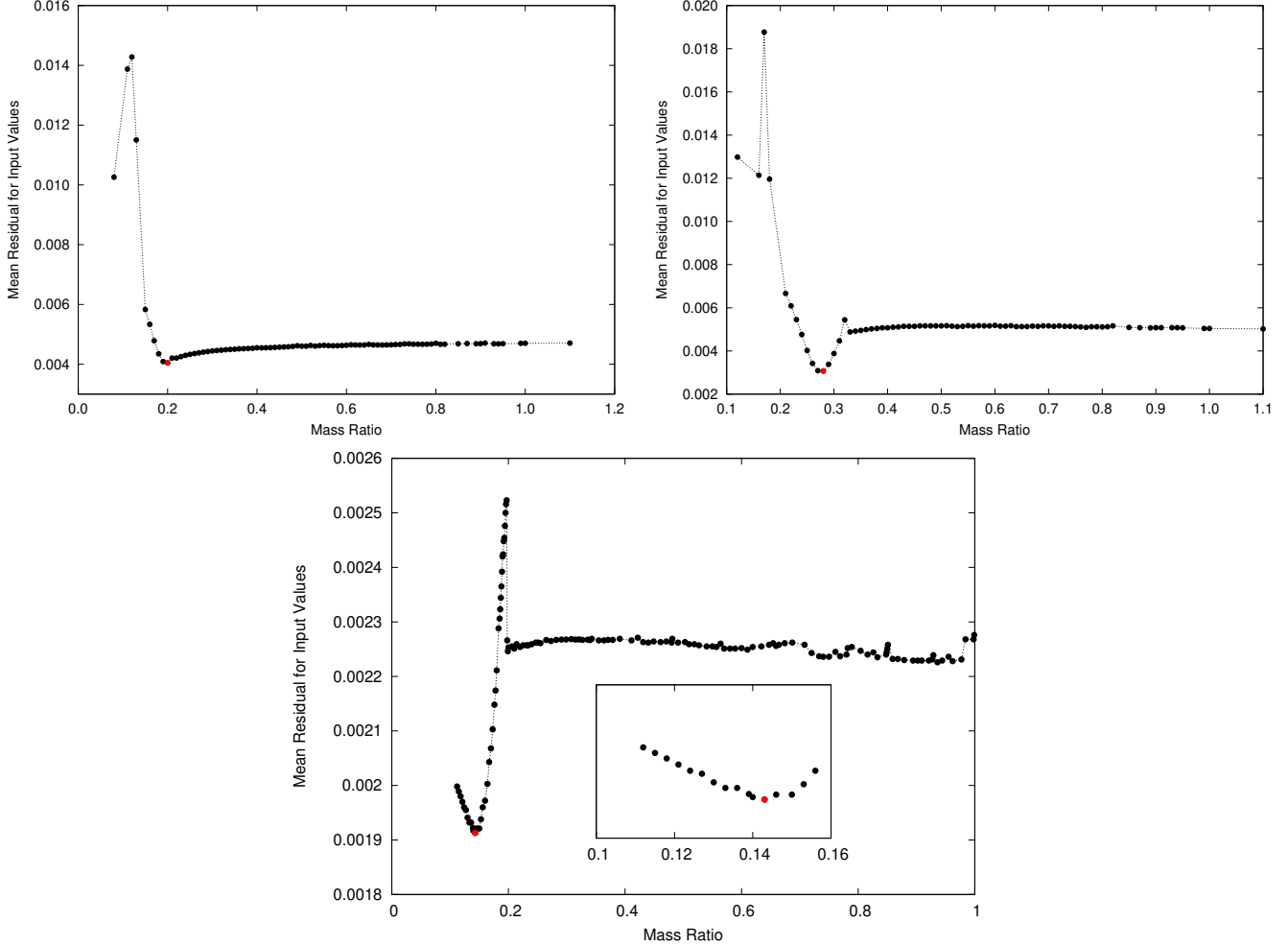


**Figure 6.** The q-search results of TIC 159102550, (top left) V1068 Her (top right) and TIC 321576458 (bottom).

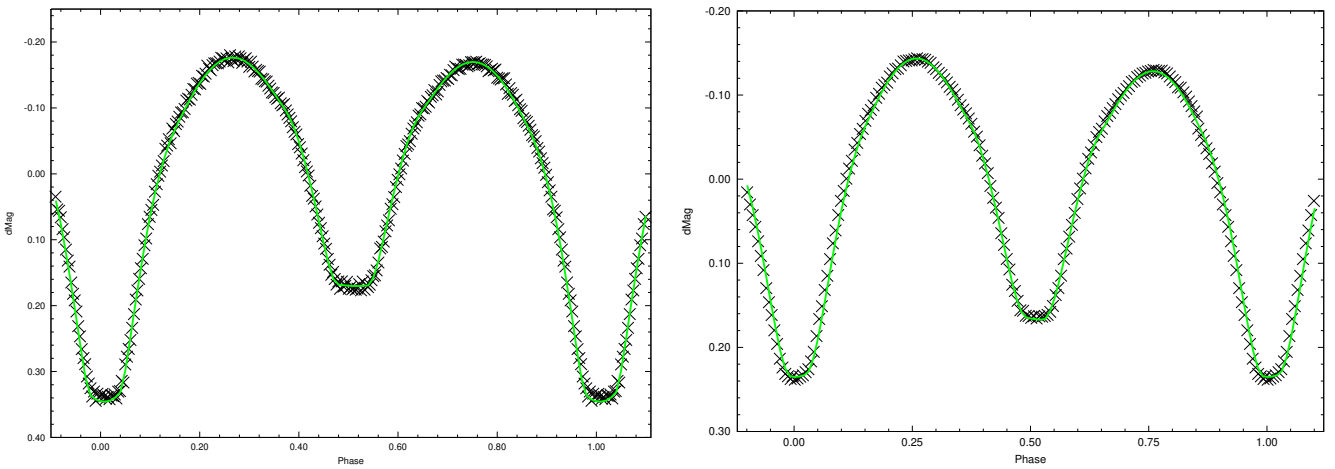


**Figure 7.** The light curve solution of TIC 159102550 (left) and V1068 Her (right). The modeled (solid green line) is superimposed over observed light curve.

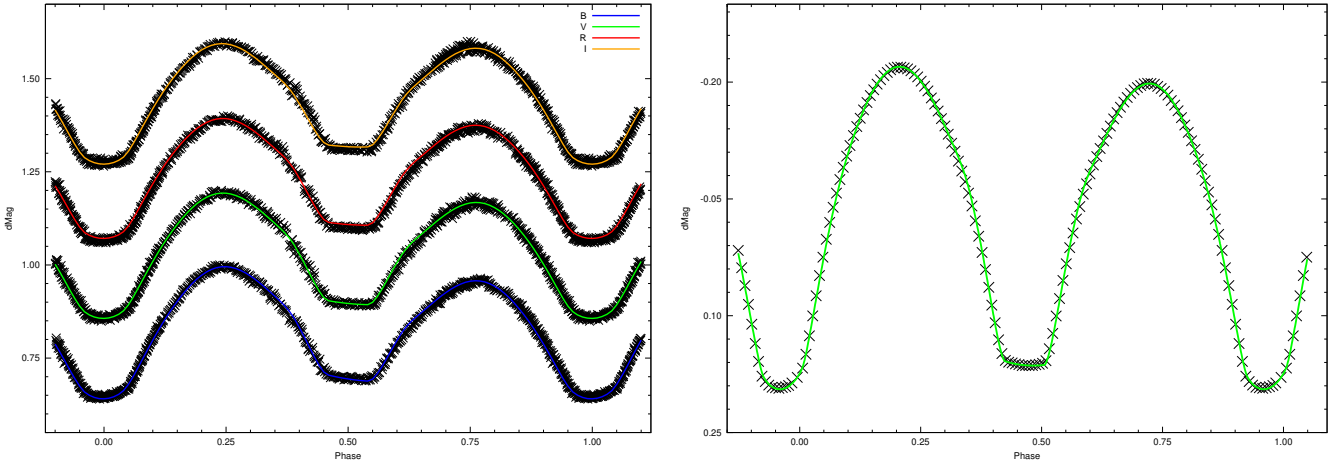
#### 4.3. MW Pav

**Table 6.** Photometric parameters of TIC 159102550 and V1068 Her

Parameters	TIC 159102550		V1068 Her	
	Without Spot	Spot	Without Spot	Spot
$q(m_2/m_1)$	0.207(4)	0.211(2)	0.322(2)	0.266(3)
$i(deg)$	77.14(4)	77.21(6)	86.47(4)	83.53(3)
$\Omega_1 = \Omega_2$	2.220(4)	2.229(8)	2.458(8)	2.364(6)
$f(\%)$	18.88	20.74	26.03	14.11
$T_1(K) (fixed)$	6109	6109	6158	6158
$T_2(K)$	5977(16)	6015(10)	5701(68)	6143(57)
$r_1(pole)$	0.492(2)	0.490(1)	0.461(1)	0.470(1)
$r_1(side)$	0.537(3)	0.535(1)	0.498(1)	0.509(1)
$r_1(back)$	0.562(3)	0.560(1)	0.528(1)	0.535(1)
$r_2(pole)$	0.242(9)	0.243(5)	0.280(3)	0.260(4)
$r_2(side)$	0.253(11)	0.254(6)	0.294(4)	0.272(5)
$r_2(back)$	0.292(23)	0.293(13)	0.339(9)	0.310(10)
$L_1/(L_1 + L_2)$	0.844(4)	0.842(2)	0.825(2)	0.824(6)
Mean Residual	0.003706	0.001926	0.001666	0.000837

The solution of Rucinski & Duerbeck (2006) suggests photometric mass-ratio of the system be  $q_{ph} = 0.122$  and  $q_{sp} = 0.228$ . They also determined the spectral type of MW Pav to be F3/IV-V. Deb & Singh (2011), uses the spectroscopic mass-ratio of Rucinski & Duerbeck (2006) and face problems in light curve fitting. However, they proposed the photometric mass-ratio of  $q = 0.200$  with a fill-out factor of 52%. More recently, Alvarez et al. (2015), presented combined light and velocity curve solution. Their UBV photometric solution suggest a new mass-ratio  $q = 0.222$  and a high fill-out factor of 60% for the system.

We have analysed the new  $BVR_cI_c$  and TESS light curves of this target. The initial value of mass ratio ( $q = 0.228$ ) and the proposed spectral type of MW Pav by Rucinski & Duerbeck (2006) help us to set the temperature of primary component at  $T_1 = 6900K$  from Cox (2000). We use this q-value and get the convergent solution in Mode-3 of the WD program. The difference in Max-I and Max-II values compelled us to determine the spot parameters. We, therefore, run a spot solution for both,  $BVR_cI_c$  and TESS, light curves. The final photometric solution is shown in Figure 8 and the parameters are listed in Table 7.

**Figure 8.** The  $BVR_cI_c$  light curve of MW Pav is shown in the left and the TESS curve is on right.

#### 4.4. TIC 321576458

**Table 7.** Photometric parameters of MW Pav

Parameters	HSH 60cm		TESS	
	Without Spot	Spot	Without Spot	Spot
$q(m_2/m_1)$	0.200(3)	0.154(1)	0.174(1)	0.175(9)
$i(deg)$	84.28(98)	80.20(40)	82.17(66)	81.79(24)
$\Omega_1 = \Omega_2$	2.167(6)	2.045(3)	2.099(13)	2.101(29)
$f(\%)$	51.53	71.57	61.00	63.20
$T_1(K)(fixed)$	6900	6900	6900	6900
$T_2(K)$	6872(97)	6987(57)	6775(143)	6838(12)
$r_1(pole)$	0.502(1)	0.523(1)	0.513(2)	0.514(5)
$r_1(side)$	0.551(1)	0.528(1)	0.567(3)	0.569(8)
$r_1(back)$	0.579(1)	0.609(1)	0.594(3)	0.596(8)
$r_2(pole)$	0.252(6)	0.237(3)	0.245(11)	0.244(2)
$r_2(side)$	0.265(8)	0.249(4)	0.258(14)	0.257(3)
$r_2(back)$	0.319(21)	0.314(15)	0.319(42)	0.317(10)
$L_1/(L_1 + L_2)_B$	0.827(4)	0.806(4)	-	-
$L_1/(L_1 + L_2)_V$	0.816(3)	0.806(3)	-	-
$L_1/(L_1 + L_2)_{R_c}$	0.814(3)	0.812(2)	-	-
$L_1/(L_1 + L_2)_{I_c}$	0.820(2)	0.822(2)	-	-
$L_1/(L_1 + L_2)_{TESS}$	-	-	0.815(1)	0.808(8)
Mean Residual	0.001889	0.001401	0.002699	0.000843

**Table 8.** Star spot parameters for TIC 159102550, V1068 Her and MW Pav

	Latitude(rad)	Longitude (rad)	Angular radius (rad)	Spot Temp. factor
TIC 159102550	4.000 <sup>a</sup>	1.600 <sup>a</sup>	0.300 <sup>a</sup>	0.850 <sup>a</sup>
V1068 Her	0.140 <sup>a</sup>	0.172(19)	1.196(55)	0.899(6)
MW Pav	2.90 <sup>a</sup>	3.95(59)	0.60 <sup>a</sup>	1.38(14)
MW Pav <sub>TESS</sub>	0.667(20)	1.409(37)	0.223(33)	0.65 <sup>a</sup>

<sup>a</sup>Assumed

a -

Since this target is also observed for the first time and no other photometric and spectroscopic mass-ratio is available in the literature. Therefore, we employed the q-search process to determine the initial mass-ratio of the system. The results are shown in Figure 6 which indicates the  $q=0.143$ . By using this q-value and keep it adjustable along with  $T_2$ ,  $\Omega_1$ ,  $i$ ,  $q$ , and  $L_1$  to get the final convergent solution. The temperature of primary component ( $T_1$ ) was taken from GAIA data. The modeled light curve fits well over the observed light curve and therefore not spot solution was performed. The fitted light curves are shown in Figure 9.

## 5. DISCUSSION AND CONCLUSION

### 5.1. TIC 159102550

By combining all times of observed primary and secondary minima, we have constructed the O-C diagrams to investigate the period changes. The O-C diagram of TIC 159102550 hints to correct the period. After period correction, we determined new values of O-C and reconstructed the diagram. The O-C for primary minima displays no large-scale change as shown in upper panel of Figure 2, which means that the revised period gives a better value than before. If we apply the same to secondary minima, it shows a different behavior as shown in below panel of Figure 2. The O-C of many targets has variable change, which include regular and irregular, such as long-term increasing and decreasing (Zhao et al. 2021; Li et al. 2022b; Zhao & Tian 2022). This can be explained by mass-transfer between both components, a third body, magnetic activities or apsidal motion (Er-gang et al. 2019; Li et al. 2022a). Sudden

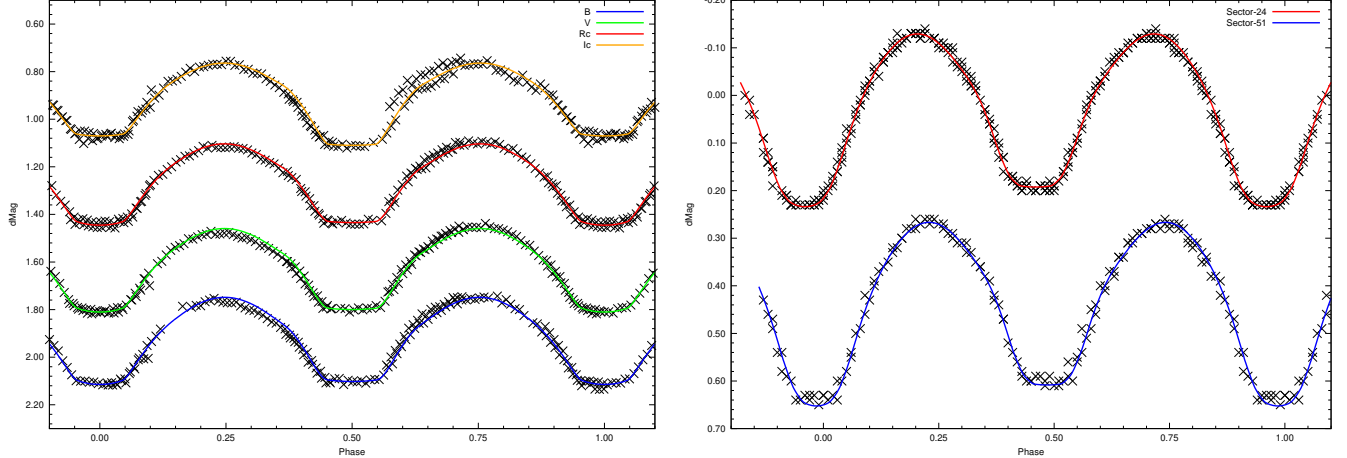


**Figure 9.** Combined light curves of TIC 321576458. The  $BVR_cI_c$  light curve of is shown in the left and the TESS curves are on right side. Solid line represents the modeled solution.

**Table 9.** Photometric parameters of MW Pav

Parameters	Sino-Thai	TESS	
	70cm telescope	Sector-24	Sector-51
$q(m_2/m_1)$	0.153(1)	0.147(1)	0.167(2)
$i(deg)$	82.57(6)	89.69(4)	88.40(1)
$\Omega_1 = \Omega_2$	2.071(4)	2.030(5)	2.082(6)
$f(\%)$	41.7	68.6	61.2
$T_1(K)(fixed)$	6140	6140	6140
$T_2(K)$	6490(116)	6001(13)	5982(25)
$r_1(pole)$	0.516(1)	0.526(1)	0.517(1)
$r_1(side)$	0.571(1)	0.585(1)	0.573(1)
$r_1(back)$	0.595(1)	0.611(1)	0.599(2)
$r_2(pole)$	0.228(3)	0.234(5)	0.239(6)
$r_2(side)$	0.238(4)	0.246(7)	0.252(7)
$r_2(back)$	0.285(10)	0.310(24)	0.309(21)
$L_1/(L_1 + L_2)_B$	0.839(1)	-	-
$L_1/(L_1 + L_2)_V$	0.836(7)	-	-
$L_1/(L_1 + L_2)_{R_c}$	0.836(5)	-	-
$L_1/(L_1 + L_2)_{I_c}$	0.815(5)	-	-
$L_1/(L_1 + L_2)_{TESS}$	-	0.844(1)	0.833(3)
Mean Residual	0.001179	0.001896	0.003015

change and even anti-correlations between the primary and secondary eclipse timing has also been reported. This anti-correlation behaviour can be explained with rapid variation in light curve due to migration of star spot over time. This phenomena can deviate the eclipse times from theoretical phase which results in different trend in O-C diagram over a small timescale (Tran et al. 2013; Zhou et al. 2019; Chang et al. 2023).

In the absence of spectroscopic parameters, absolute values of binary components cannot be determined directly. However, if we assume that the primary component is a main-sequence star, then we can estimate the mass of secondary component from Cox (2000). The absolute parameters are tabulated in Table 10. The photometric solution suggest that system is an A-type low mass-ratio ( $q = 0.211(2)$ ) contact binary with a weak degree of contact (20.74%). It's secondary component is an evolved star while the more massive primary is still on the main-sequence as shown in Figure 10. We suggest continuous monitoring of this target.

### 5.2. V1068 Her

The period investigation of V1068 Her suggest that binary is going through increase in period by  $dP/dt = 1.247(9) \times 10^{-7} \text{ days/yr}$ . The continuous increase in period indicates that binary is undergoing a process of mass transfer from less massive secondary to more massive primary component. We can use the well-known equation (Singh & Chaubey 1986; Carroll & Ostlie 2017)

$$\frac{dP/dt}{P} = 3 \frac{dM_2}{dt} \left( \frac{1}{M_2} - \frac{1}{M_1} \right) \quad (5)$$

and determine the mass transfer rate of  $4.304(5) \times 10^{-8} M_{\odot} \text{ yr}^{-1}$  at thermal time-scale of  $6.481(5) \times 10^6 \text{ yr}$  for V1068 Her.

Since no absolute parameters of this target was previously published, so we have estimated the mass of primary component from Cox (2000). All the parameters are listed in Table 10. The photometric solution indicates the mass-ratio of  $q = 0.266(3)$  and shallow degree of contact ( $f = 14.11\%$ ). The system lies in A-subtype category of contact binaries. Its more massive primary component is a main-sequence star while the less massive secondary companion is an evolved star. With the transfer of mass from secondary to primary component, the mass-ratio of the system will further decrease. If the mass transfer process is conservative, the period change of V1068 Her suggests that the system will oscillate around a critical mass-ratio. Since both component of binary are in thermal contact ( $\Delta T = 15K$ ), they may not be oscillating between contact and semi-detached state. When the mass-ratio decreases to critical value the period will decrease which indicates the reversal in mass transfer direction. Therefore, the mass-ratio will start increasing and as soon as it increases the critical value, the period of V1068 Her will start increasing again and the system will keep on oscillating. A critical AML rate will keep the V1068 Her in shallow contact stage. The larger AML rate will make the stars to reach at the outer Lagrangian point ( $L_2$ ) before merger into a single star (Rahunen 1981; Qian 2003; Qian et al. 2013).

### 5.3. MW Pav

The long term period analysis of MW Pav indicates the increase in period by  $2.220(9) \times 10^{-7} \text{ days/yr}$ . The continuous increase in period indicates that both systems are undergoing a process of mass transfer from less massive secondary to more massive primary component. We have used the Equation 5 and determined that system is transferring the mass from less massive secondary to more massive primary component at the rate of  $2.307(6) \times 10^{-8} M_{\odot} \text{ yr}^{-1}$  in thermal time-scale of  $1.11(4) \times 10^7 \text{ yr}$ .

The  $BVR_cI_c$  light curve analysis shows that system is a W-subtype low mass-ratio ( $q = 0.154(1)$ ) contact binary in deep contact stage ( $f = 71.57\%$ ). However, light curve solution of TESS data put it in A-subtype category. It is possible that binary has now changed from W-type to A-type contact system. Such phenomena has also been reported by Qian & Yang (2005) and Qian et al. (2008). We have opted the radial velocity data from Rucinski & Duerbeck (2006) and combined it with our photometric solution to determine the absolute parameters of MW Pav. They are presented in Table 10. With the increase in period and the transfer of mass from secondary to primary component, the mass-ratio of the system will further decrease. The increasing period will widen the orbit, however, the strong degree of contact, (71.51%) for HSH observations and (63.20%) for TESS, will hold the binary in contact configuration for a longer duration of time until the Hut's criteria (Hut 1980) is achieved ( $J_{\text{orbital}} \leq 3J_{\text{spin}}$ ). The MW Pav will eventually evolve into single rapidly rotating star.

### 5.4. TIC 321576458

The O-C diagram of this target (Figure 5) does not hint of any period variation during the short time span, therefore, period change and mass transfer rate cannot be determined. Assuming that the primary component is a main-sequence star, we have estimated the absolute parameter from Cox (2000) and shown in Table 10. The photometric solution suggest that system is an W-type low mass-ratio ( $q = 0.153(1)$ ) with moderate fill-out factor of 41.7%. However, TESS light curve analysis put it in A-type category with higher contact degree of 61.2%. It's secondary component is an evolved star while the more massive primary is still on the main-sequence as shown in Figure 10. More times of primary and secondary minima will help to study the orbital period in detail. We suggest to monitor the target for a longer duration.

### 5.5. Statistics on some low mass ratio binaries

**Table 10.** Absolute parameters four contact binaries

System	$M_1$	$M_2$	$R_1$	$R_2$	$L_1$	$L_2$	a
TIC 159102550	$1.400M_\odot$	$0.295M_\odot$	$1.633R_\odot$	$0.817R_\odot$	$4.535L_\odot$	$0.783L_\odot$	$3.104R_\odot$
V1068 Her	$1.050M_\odot$	$0.279M_\odot$	$1.252R_\odot$	$0.696R_\odot$	$2.022L_\odot$	$0.618L_\odot$	$2.482R_\odot$
MW Pav	$1.670M_\odot$	$0.257M_\odot$	$2.481R_\odot$	$1.193R_\odot$	$12.518L_\odot$	$3.043L_\odot$	$4.485R_\odot$
TIC 321576458	$1.200M_\odot$	$0.183M_\odot$	$1.417R_\odot$	$0.632R_\odot$	$2.561L_\odot$	$0.637L_\odot$	$2.527R_\odot$

During recent years, many authors have paid much attention to the statistical studies on contact binary systems. The analysis of orbital period distribution of several authors (e.g., (Lucy 1976), (Rucinski 2007)) showed a strong and sharp peak at nearly 0.22 days which is considered as short-period limit for contact binaries. Qian et al. (2017), through investigation of more than 40,000 systems reported 0.29 days and Li et al. (2020) established 0.30 days while analyzing 446 systems. Not only this, Eggen (1967), established an important period-color relationship for contact binaries which helped to the model of thermal relaxation oscillation theory. Yang & Qian (2015) also performed statistical analysis on the evolutionary scenarios of contact binary systems but his analysis was limited to deep contact binaries. We have discussed the distribution of low mass-ratio contact binary systems on the Mass-Luminosity (ML) diagram to study their evolutionary track. We have also calculated their initial mass, age and momentum ratio of these system. We have collected absolute parameters of 122 contact binaries, including our present study, to understand the evolutionary scenario of our target binaries. The data contains 47 extreme low mass-ratio (ELMR) binaries with  $q \leq 0.100$  tabulated in Table 11 and 75 low mass-ratio (LMR) binaries with  $q = 0.10 - 0.25$  listed in Table 12.

**Table 11.** Absolute parameters of extreme low mass-ratio contact binaries

Star	$q$ ( $m_2/m_1$ )	$P$ (d)	$dP/dt$ ( $\times 10^{-7}$ d)	$f$ (%)	$i$ ( $^{\circ}$ )	$T_1$ (K)	$T_2$ (K)	$M_1$ ( $M_{\odot}$ )	$M_2$ ( $M_{\odot}$ )	$R_1$ ( $R_{\odot}$ )	$R_2$ ( $R_{\odot}$ )	$L_1$ ( $L_{\odot}$ )	$L_2$ ( $L_{\odot}$ )	$a$ ( $R_{\odot}$ )	Ref.
V1187 Her	0.044	0.310760	-1.5	80.00	65.90	6250	6651	1.200	0.050	1.370	0.380	2.570	0.254	2.076	Caton et al. (2019)
TYC 4002-2628-1	0.048	0.367058	0.0162	5.00	69.90	6032	6044	1.110	0.054	1.450	0.390	2.497	0.182	2.265	Guo et al. (2022)
VSX J082700.8+462850	0.055	0.277158	-9.52	19.00	68.70	5870	5828	1.060	0.060	1.150	0.320	1.409	0.106	1.854	Li et al. (2021a)
IP Lyn	0.055	0.489115	3.82	21.40	75.54	6677	6410	1.903	0.105	2.070	0.586	7.641	0.520	3.289	Yin et al. (2023)
KIC 4244929	0.059	0.341403	-	81.00	70.60	5857	5867	1.481	0.087	1.521	0.477	2.443	0.242	2.384	Şenavci et al. (2016)
KIC 9151972	0.059	0.386796	-	76.00	70.10	6040	5982	1.606	0.095	1.696	0.528	3.435	0.320	2.662	Şenavci et al. (2016)
ASAS J083241+2332.4	0.065	0.311300	8.85	50.65	82.74	6300	6667	1.220	0.080	1.340	0.420	2.538	0.313	2.106	Sriram et al. (2016)
V857 Her	0.065	0.382231	2.9	83.80	85.43	8300	8513	2.180	0.142	1.854	0.616	14.636	1.788	2.929	Qian et al. (2005b)
KIC 8539720	0.067	0.744499	-	47.00	71.10	6351	5972	2.438	0.163	2.955	0.929	12.747	0.985	4.745	Şenavci et al. (2016)
CW Lyn	0.067	0.812401	-	-	77.50	6532	6284	1.680	0.110	2.810	0.960	12.897	1.289	4.440	Selam (2004)
ASAS J104422-0711.2	0.073	0.611711	-	83.00	72.70	7200	7190	1.480	0.110	2.210	0.760	11.776	1.385	3.533	Wadhwa et al. (2023)
KIC 3127873	0.073	0.671526	-	65.00	80.50	6069	5791	2.268	0.166	2.690	0.899	8.808	0.815	4.333	Şenavci et al. (2016)
KIC 12352712	0.073	0.722065	-	57.00	82.50	6667	6399	2.377	0.174	2.859	0.944	14.489	1.341	4.619	Şenavci et al. (2016)
NSVS 2569022	0.077	0.287797	-	1.40	76.29	6100	6100	1.170	0.090	1.190	0.380	1.759	0.179	1.977	Kjurkchieva et al. (2018a)
ZZ Psa	0.078	0.374050	-	97.00	75.25	6514	6703	1.213	0.095	1.422	0.559	3.266	0.566	2.385	Wadhwa et al. (2020)
SX Crv	0.079	0.316638	-	27.00	61.21	6340	6160	1.246	0.098	1.347	0.409	2.630	0.216	2.153	Zoli et al. (2004)
V53	0.079	0.308449	0.589	60.40	74.80	7415	6791	1.472	0.115	1.383	0.481	5.188	0.441	2.237	Li et al. (2017)
CRTS J224827.6 + 341351	0.079	0.321026	77.1	91.60	83.20	6077	5541	1.233	0.098	1.350	0.456	2.230	0.176	2.166	Liu et al. (2023)
AW UMa	0.080	0.438700	-2.05	80.20	80.60	7175	7110	1.790	0.140	1.880	0.660	8.404	0.999	3.019	Yang (2008)
KIC 10007533	0.081	0.648064	-	54.00	80.70	6808	6338	2.199	0.178	2.566	0.881	12.691	1.124	4.198	Şenavci et al. (2016)
CRTS J155009.2 + 493639	0.082	0.460910	6.22	18.90	85.70	6619	6199	1.599	0.130	1.882	0.644	6.100	0.549	3.008	Liu et al. (2023)
V870 Ara	0.082	0.399722	-	96.40	70.00	5860	6210	1.503	0.123	1.670	0.610	2.951	0.496	2.680	Szalai et al. (2007)
KIC 8145477	0.082	0.565784	-	40.00	82.00	6801	6473	2.012	0.165	2.260	0.767	9.804	0.927	3.724	Şenavci et al. (2016)
CRTS J234634.7 + 222824	0.086	0.290693	2.19	37.30	74.60	5851	5746	1.141	0.098	1.218	0.425	1.560	0.177	1.980	Liu et al. (2023)
TYC 835-1081-1	0.086	0.448058	-	66.00	80.15	6720	6480	1.470	0.130	1.760	0.630	5.668	0.628	2.870	Wadhwa et al. (2022)
CRTS J154254.0 + 324652	0.087	0.354988	-8.44	94.30	84.40	5885	6067	1.317	0.114	1.464	0.514	2.307	0.321	2.373	Liu et al. (2023)
KIC 11144556	0.087	0.642980	-	73.00	69.70	6428	6202	2.174	0.191	2.542	0.927	9.898	1.141	4.169	Şenavci et al. (2016)
KIC 10596883	0.088	0.468911	-	18.00	69.90	7296	6514	1.772	0.156	1.882	0.641	9.005	0.664	3.155	Şenavci et al. (2016)
CRTS J155106.5 + 303534	0.089	0.380989	-5.13	69.30	74.80	7147	6819	1.384	0.122	1.559	0.552	5.690	0.591	2.530	Liu et al. (2023)
1SWASP J132829.37+555246.1	0.089	0.384705	-4.46	70.00	81.50	6300	6319	1.230	0.110	1.490	0.550	3.138	0.433	2.449	Li et al. (2021a)
ASAS J103373-3709.5	0.090	0.343402	11.5	57.00	68.10	6050	5741	1.180	0.110	1.360	0.490	2.223	0.234	2.242	Wadhwa et al. (2023)
KIC 8804824	0.091	0.457404	-	14.00	81.00	7202	6168	1.738	0.158	1.829	0.628	8.075	0.512	3.086	Şenavci et al. (2016)
KIC 5374883	0.092	0.419717	-	71.66	65.92	5800	5679	1.540	0.140	1.720	0.620	3.004	0.359	2.799	Li et al. (2020)
KR Com	0.093	0.407968	-	99.00	54.40	5920	6130	0.880	0.080	1.445	0.505	2.301	0.323	2.279	Gazeas et al. (2021)
CRTS J170307.9 + 020101	0.093	0.290984	2.54	69.80	75.70	5433	5237	1.134	0.105	1.204	0.436	1.133	0.128	1.980	Liu et al. (2023)
CRTS J223837.9 + 321932	0.093	0.444170	5.28	44.90	74.00	6919	6756	1.541	0.144	1.784	0.646	6.544	0.780	2.910	Liu et al. (2023)
KIC 7698650	0.095	0.599155	-	61.00	79.10	6107	6026	2.064	0.196	2.357	0.876	6.933	0.908	3.917	Şenavci et al. (2016)
CRTS J164000.2 + 491335	0.095	0.390782	-3.19	28.70	83.50	7137	6574	1.402	0.133	1.580	0.577	5.811	0.558	2.590	Liu et al. (2023)
ASAS J153433+1225.3	0.096	0.330057	6.8	56.10	78.80	6079	6060	1.470	0.140	1.410	0.530	2.436	0.340	2.351	Li et al. (2022)
CSS J233332.9+180430	0.096	0.628784	-298	37.40	82.50	6770	6379	2.030	0.200	2.400	0.870	10.856	1.124	4.027	Li et al. (2022)
FP Boo	0.096	0.640482	-	38.00	68.80	6980	6456	1.614	0.154	2.310	0.774	11.364	0.934	6.290	Gazeas et al. (2006)
KIC 11097678	0.097	0.999716	-	87.00	85.14	6493	6426	0.960	0.189	3.897	1.264	24.218	2.444	4.398	Şenavci et al. (2016)
CRTS J162327.1 + 031900	0.097	0.474562	-	27.40	82.50	6914	6380	1.612	0.156	1.888	0.695	7.308	0.718	3.090	Liu et al. (2023)
CRTS J133031.1 + 161202	0.098	0.302666	-	56.00	88.30	5860	6019	1.162	0.114	1.237	0.459	1.619	0.248	2.054	Liu et al. (2023)
KIC 9453192	0.099	0.718837	-	44.00	76.90	6729	6218	2.314	0.229	2.734	1.010	13.750	1.368	4.600	Şenavci et al. (2016)
NSVS 4701980	0.099	0.355763	-34.4	55.30	87.40	5892	6075	1.510	0.150	1.510	0.590	2.465	0.425	2.497	Li et al. (2022)
CRTS J160755.2 + 332342	0.099	0.357288	-	36.10	74.90	7987	7476	1.310	0.130	1.445	0.537	7.624	0.808	2.388	Liu et al. (2023)

**Table 12.** Absolute parameters of low mass-ratio contact binaries

Star	$q$ ( $m_2/m_1$ )	$P$ (d)	$dP/dt$ ( $\times 10^{-7}$ d)	$f$ (%)	$i$ ( $^{\circ}$ )	$T_1$ (K)	$T_2$ (K)	$M_1$ ( $M_{\odot}$ )	$M_2$ ( $M_{\odot}$ )	$R_1$ ( $R_{\odot}$ )	$R_2$ ( $R_{\odot}$ )	$L_1$ ( $L_{\odot}$ )	$L_2$ ( $L_{\odot}$ )	$a$ ( $R_{\odot}$ )	Ref.
NW Aps	0.100	1.065550	-	45.00	85.10	6640	6229	1.400	0.140	2.556	0.946	11.394	1.209	5.060	Wadhwa (2005)
AW CrB	0.101	0.360900	3.58	75.00	82.10	6700	6808	1.390	0.140	1.480	0.580	3.960	0.648	2.453	Broens (2013)
DN Boo	0.103	0.447568	-	64.00	60.02	6095	6071	1.428	0.148	1.710	0.670	3.621	0.547	2.860	Şenavci et al. (2008)
ASAS J082243+1927.0	0.106	0.280000	-	72.00	76.58	5960	6078	1.100	0.170	1.150	0.420	1.497	0.216	1.947	Kandulapati et al. (2015)
V1191 Cyg	0.107	0.313400	4.5	68.60	80.40	6500	6626	1.310	0.140	1.310	0.520	2.748	0.468	2.193	Ulaş et al. (2012)
CK Boo	0.109	0.355200	0.98	65.00	64.90	6200	6291	1.430	0.160	1.440	0.560	2.749	0.441	2.459	Yang et al. (2012)
NSVS 10368868	0.110	0.287160	10	61.00	78.00	5963	6202	1.390	0.150	1.250	0.490	1.772	0.319	2.111	Li et al. (2022)
TYC 6995-813-1	0.111	0.383180	-	72.00	84.03	6300	6235	1.230	0.135	1.460	0.600	3.013	0.488	2.458	Wadhwa et al. (2021)
ATO J022.8782+55.2989	0.111	0.378150	-	4.50	71.75	6400	6300	1.320	0.150	1.430	0.531	3.078	0.399	2.500	Kjurkchieva et al. (2018b)
FG Hya	0.112	0.327800	-1.96	85.60	82.30	5900	6012	1.450	0.160	1.400	0.580	2.131	0.394	2.340	Qian & Yang (2005)
CSS J110658.4+511201	0.119	0.400968	67	92.00	86.40	6224	6291	1.560	0.180	1.650	0.700	3.666	0.689	2.747	Li et al. (2022)
ASASSN-V J022733.60+360447.1	0.120	0.413965	8.5	58.30	74.60	6494	6374	1.580	0.190	1.650	0.680	4.344	0.685	2.822	Li et al. (2022)
V2787 Ori	0.120	0.810980	-	18.10	84.74	6993	5418	1.440	0.170	2.450	0.960	12.879	0.713	4.290	Tian et al. (2019)
V0566 Cam	0.121	0.444062	56.8	20.30	73.10	7037	6642	1.630	0.200	1.710	0.670	6.433	0.784	2.990	Li et al. (2022)
GR Vir	0.122	0.346979	-4.32	78.60	83.36	6300	6163	1.370	0.170	1.420	0.610	2.850	0.482	2.395	Qian & Yang (2004)
NSVS 6798913	0.128	0.362541	41	57.30	87.50	6029	6071	1.480	0.190	1.470	0.620	2.562	0.469	2.534	Li et al. (2022)
NSVS 7480723	0.128	0.299294	11.5	45.20	85.50	5822	5810	1.380	0.180	1.260	0.520	1.637	0.276	2.180	Li et al. (2022)
eps CrA	0.128	0.591440	4.67	25.00	74.00	6678	6341	1.700	0.230	2.100	0.850	7.869	1.048	3.690	Yang et al. (2005b)
ASAS0154+20	0.137	0.472488	-	16.00	79.90	6680	6011	1.916	0.263	1.858	0.768	6.167	0.691	3.303	Popov & Petrov (2022)
V584 Cam	0.137	0.464699	-	33.00	68.42	5573	5321	1.546	0.212	1.754	0.728	2.663	0.381	3.041	Martignoni et al. (2021)
V345 Gem	0.142	0.274800	0.59	73.30	72.90	6115	6365	1.060	0.150	1.100	0.500	1.518	0.368	1.892	Yang et al. (2009)
NSVS 3650324	0.142	0.379297	50.6	96.30	77.80	6590	6463	1.490	0.210	1.550	0.720	4.065	0.812	2.627	Li et al. (2022)
V410 Aur	0.143	0.366400	8.22	52.40	84.00	6040	5915	1.300	0.190	1.400	0.610	2.340	0.409	2.456	Yang et al. (2005a)
V710 Mon	0.143	0.405200	1.95	62.70	79.90	6145	6294	1.140	0.160	1.460	0.660	2.727	0.613	2.512	Liu et al. (2014)
ASAS J142124+1813.1	0.144	0.242720	-	23.00	79.79	6160	6970	3.144	0.453	1.403	0.597	2.543	0.755	2.510	Michel & Kjurkchieva (2019)
TIC 89428764	0.147	0.376610	6.36	32.70	76.90	7070	6797	1.500	0.220	1.470	0.630	4.844	0.760	2.630	Tang et al. (2022)
XY LMi	0.148	0.436900	-1.67	74.10	81.00	6144	6093	1.180	0.180	1.540	0.710	3.032	0.623	2.679	Qian et al. (2011)
EM Psc	0.149	0.343959	39.7	95.30	88.60	5300	4987	1.050	0.156	1.283	0.631	1.165	0.221	2.195	Qian et al. (2008)
NX Cam	0.150	0.605771	-	54.60	82.36	6655	6015	1.750	0.262	2.025	0.839	7.225	0.827	3.796	Martignoni et al. (2021)
NSVS 5029961	0.151	0.376666	-	33.80	77.30	6260	6206	1.872	0.284	1.573	0.680	3.409	0.615	2.830	Zheng et al. (2021)
TIC 321576458	0.153	0.376145	-	41.70	82.57	6140	6490	1.200	0.183	1.417	0.632	2.560	0.636	2.438	This study
MW Pav	0.154	0.794997	-	71.50	80.20	6900	6987	1.670	0.257	2.481	1.193	12.518	3.043	4.485	This study
NSVS 2643686	0.158	0.396068	-	72.90	81.31	5905	5840	1.309	0.200	1.536	0.721	2.574	0.543	2.602	Martignoni et al. (2021)
HV Aqr	0.159	0.374455	-1.29	56.21	78.22	5915	5948	1.050	0.160	1.320	0.580	1.914	0.378	2.325	Zubairi et al. (2023)
V728 Her	0.160	0.471300	1.92	81.00	86.70	6585	6678	1.800	0.280	1.870	0.820	5.899	1.200	3.247	Erkan & Ulaş (2016)
CRTS J163819.6+03485	0.160	0.205332	-0.711	63.00	88.50	6696	6502	1.190	0.190	0.930	0.440	1.560	0.310	1.628	Papageorgiou et al. (2023)
NSVS 1926064	0.160	0.407472	-	70.90	78.40	6020	5923	1.558	0.249	1.605	0.755	3.035	0.629	2.812	Kjurkchieva et al. (2020)
V144	0.160	0.721590	-	19.50	76.57	7120	6808	1.310	0.210	2.230	0.950	11.466	1.739	3.890	Li & Qian (2013)
NSVS 2256852	0.161	0.348890	-2.36	17.30	75.60	6804	5606	0.950	0.150	1.180	0.520	2.677	0.240	2.160	Kjurkchieva et al. (2018c)
TIC 393943031	0.163	0.449793	4.21	50.80	81.60	6460	6270	1.400	0.230	1.620	0.750	4.101	0.780	2.910	Tang et al. (2022)
AH Aur	0.165	0.494109	-7.75	75.00	76.10	6200	6418	1.674	0.283	1.897	0.837	4.771	1.066	3.284	Gazeas et al. (2005)
TV Mus	0.166	0.445675	-2.16	74.30	77.15	5980	5808	1.350	0.220	1.700	0.830	3.316	0.703	2.848	Qian et al. (2005a)
AH Cnc	0.168	0.360440	3.99	58.50	90.00	6300	6265	1.100	0.190	1.299	0.619	2.385	0.530	2.316	Zhang & Deng (2005); Qian et al. (2006)
NSVS 13602901	0.171	0.523790	-	44.00	83.59	6250	6222	1.190	0.203	1.690	0.790	3.710	0.839	3.048	Wadhwa et al. (2021)
CIU Tau	0.177	0.412537	-18.1	50.10	73.95	5900	5938	1.200	0.210	1.445	0.695	2.270	0.539	2.610	Qian et al. (2005a)
V458 Mon	0.183	0.396952	3.69	29.50	82.68	6144	6067	1.200	0.219	1.379	0.655	2.431	0.522	2.549	Zubairi et al. (2023)
TY Pup	0.184	0.819240	0.557	84.30	83.63	6900	6915	1.650	0.303	2.636	1.373	14.131	3.867	4.597	Sarotsakulchais et al. (2018)
GV Leo	0.188	0.266730	-4.95	17.74	76.13	4850	5344	1.010	0.190	1.010	0.490	0.506	0.176	1.850	Kriwattanawong & Poojan (2013)
BO Ari	0.190	0.318190	-2.81	49.80	81.91	5940	5908	0.995	0.189	1.090	0.515	1.327	0.290	2.071	Girol et al. (2015)
EK Aqr	0.192	0.612802	3.63	32.80	76.38	7000	6808	1.795	0.345	2.113	1.030	15.603	2.045	3.905	Gao et al. (2022a)
Y Sex	0.195	0.419810	0.46	50.80	77.67	6400	6211	1.559	0.305	1.589	0.799	3.801	0.852	2.898	Yang et al. (2021)
CSS J022914.4+044340	0.198	0.306139	-	63.70	88.40	5855	5747	1.440	0.290	1.260	0.650	1.674	0.414	2.290	Li & Li (2021)
V402 Aur	0.201	0.603500	-	3.00	52.65	6700	6775	1.638	0.327	0.915	1.997	1.514	7.538	3.770	Zola et al. (2004)
V1363 Ori	0.205	0.431924	1.56	56.60	56.90	6156	5627	1.181	0.242	1.470	0.736	2.784	0.487	2.699	Yang et al. (2021)
DN Aur	0.205	0.616889	-	46.10	76.88	6830	6750	1.440	0.295	1.983	1.016	7.677	1.923	3.657	Godfrey et al. (1996)
HI Pup	0.206	0.432620	-	20.00	82.20	6500	6377	1.220	0.230	1.440	0.670	3.321	0.666	2.720	Ulaş & Ulusoy (2014)
V429 Cam	0.208	0.441160	6.97	37.90	81.50	6366	6287	1.360	0.280	1.550	0.780	3.540	0.853	2.870	Li et al. (2021b)
TIC 159102550	0.211	0.488239	-	20.74	77.21	6109	6015	1.400	0.295	1.633	0.817	3.332	0.784	3.105	This study
NS Cam	0.213	0.907390	-2.25	17.00	85.00	6250	5689	1.180	0.250	2.360	1.160	7.625	1.265	4.450	Samec et al. (2020)
V409 Hya	0.216	0.472270	5.41	60.60	89.46	7000	6730	1.500	0.330	1.696	0.903	6.196	1.501	3.116	Ni et al. (2014)
V830 Cep	0.228	0.260133	-0.85	26.20	88.60	6021	6147	1.840	0.190	0.910	0.470	0.976	0.283	1.729	Li et al. (2021a)
YY Crb	0.232	0.376564	-	23.00	79.50	6100	6499	1.393	0.339	1.38					

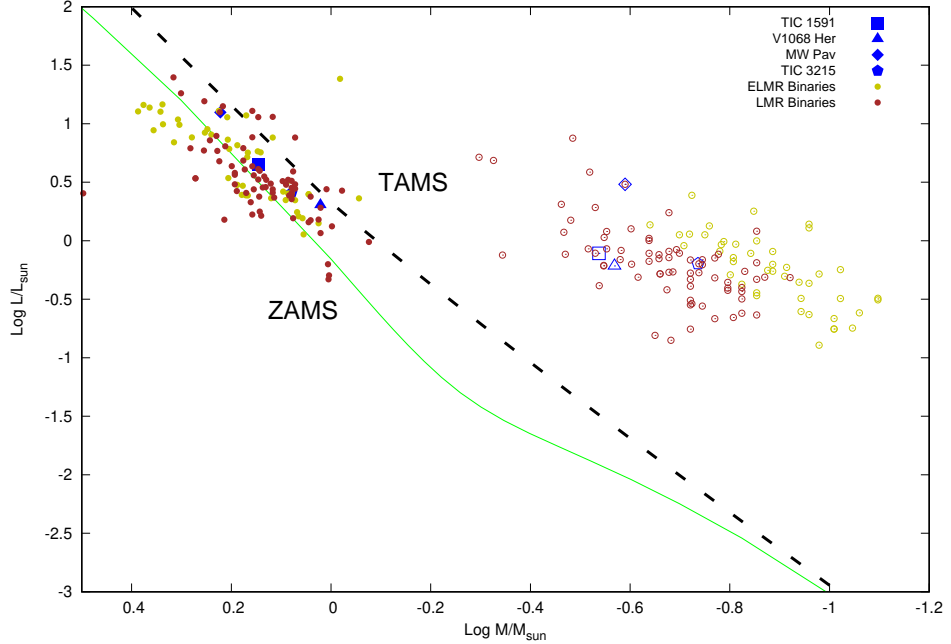


**Figure 10.** The mass-luminosity diagram of low mass ratio contact binaries. The solid symbols represents the primary components and the hollow are secondary components. Symbols with blue color shows our targets.

We have employed the model proposed by Yıldız & Doğan (2013) to calculate the initial mass of both components. We have computed the initial mass of secondary component ( $M_{2i}$ ) in terms of its higher luminosity for present mass using Equation 6, with  $M_2$  as the present mass of secondary and  $M_{L2}$  as  $(L_2/1.49)^{1/4.216}$  in solar units. The initial mass of the primary component  $M_{1i}$  is calculated by using  $\gamma = 0.6640$ , the same value as used by Yıldız & Doğan (2013). In order to calculate the age of our sample stars we have used the following equations 7 and 8. We have also compared our target with other low mass ratio binaries. The values of their initial masses are tabulated in Table 13

$$M_{2i} = M_2 + 2.50 \times (M_{L2} - M_2 - 0.07)^{0.64}, \quad (6)$$

$$M_{2mean} = \frac{M_{2i} + M_{L2}}{2} \quad (7)$$

$$\tau_{MS} = \frac{10}{(M/M_\odot)^{4.05}} \times \left[ 0.00560 \times \left( \frac{M}{M_\odot} + 3.993 \right)^{3.16} + 0.042 \right] Gyr \quad (8)$$

For these binaries the ratio of spin angular momentum ( $J_s$ ) and orbital angular momentum ( $J_o$ ) is calculated using the equation 9 provided by Yang & Qian (2015) and is listed in Table 13

$$\frac{J_s}{J_o} = \frac{1+q}{q} (k_1^2 r_1^2 + q k_2^2 r_2^2), \quad (9)$$

The value of gyration radii ( $k_1^2 = k_2^2 = k^2$ ) was opted from (Li & Zhang 2006) as 0.06. The ratio of spin and orbital angular momentum indicates that all LMR, including our targets, are in dynamically stable state. However, a few of the ELMR binaries have crossed the threshold value of 1/3. According to Li et al. (2021a), the most likely reason of this, is that the gyration radii (k) must be lower than 0.06. This means that the limit of mass ratio of contact binaries is affected by  $k^2$ .

If we keep the system V1187 Her exactly at the stability limit, then the value of  $k^2$  is 0.03214. The relation between q and spin-orbital angular momentum ratio is shown in figure 11. The fitting function is shown in Equation 10.

$$\frac{J_s}{J_o} = 0.052(\pm 0.002) + 0.64(\pm 0.02) \times e^{-21.15(\pm 0.48) \times q} \quad (10)$$

Based on our samples, the updated relationship between mass ratio and spin-orbital angular momentum ratio gives us a new value of  $q_{min} = 0.0388$  for Darwin's stability in contact binaries.

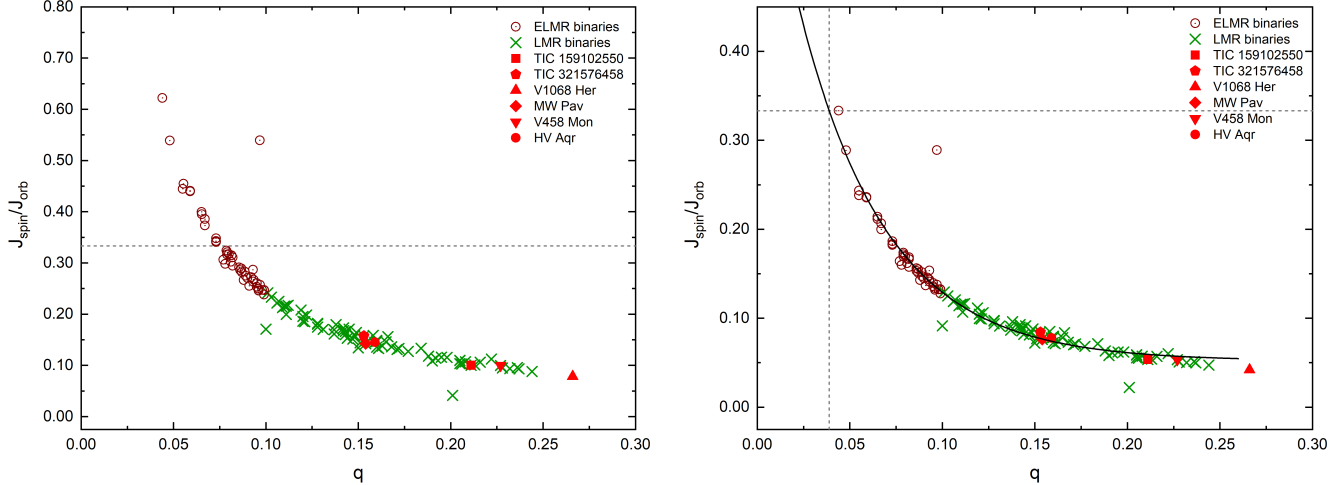


**Figure 11.** The relationship with mass ratio and  $J_s/J_o$ . The horizontal dashed line represents critical value for Darwin's stability. Left Figure shows the values with  $k^2 = 0.06$  and right one with  $k^2 = 0.03214$

## 6. ACKNOWLEDGMENTS

This study is partly supported by the National Natural Science Foundation of China (Grant Nos. 11933008), Yunnan Natural Science Foundation (No. 202001AT070051) and Yunnan Revitalization Talent Support Program Young Talent Project. Some data of Present study is from LAMOST, which is operated and managed by the National Astronomical Observatories, Chinese Academy of Sciences. This work also used TESS and GAIA data and authors thanks a lot for the team of TESS and GAIA. This research has also made use of the International Variable Star Index (VSX) database, operated at AAVSO, Cambridge, Massachusetts, USA.

**Table 13.** Momentum ratio, and initial mass of primary and secondary components of selected binary systems

Star	q	$J_{spin}/J_{orb}^*$	$J_{spin}/J_{orb}$	$M_{2i}$	$M_{1i}$	Age
V1187 Her	0.044	0.3309	0.6147	1.737	0.633	6.63
TYC 4002-2628-1	0.048	0.2901	0.5389	1.586	0.595	9.12
VSX J082700.8+462850	0.055	0.2393	0.4446	1.471	0.586	11.88
IP Lyn	0.055	0.2448	0.4546	1.918	1.294	4.58
KIC 4244929	0.059	0.2375	0.4411	1.676	0.947	7.35
KIC 9151972	0.059	0.2367	0.4398	1.757	1.048	6.22
ASAS J083241+2332.4	0.065	0.2151	0.3996	1.694	0.678	7.12
V857 Her	0.065	0.2126	0.3949	2.365	1.433	2.23
KIC 8539720	0.067	0.2008	0.3731	2.102	1.786	3.28
CW Lyn	0.067	0.2076	0.3857	2.254	0.960	2.64
ASAS J104422-0711.2	0.073	0.1874	0.3481	2.282	0.750	2.54
KIC 3127873	0.073	0.1845	0.3427	2.026	1.643	3.70
KIC 12352712	0.073	0.1833	0.3406	2.219	1.690	2.73
NSVS 2569022	0.077	0.1649	0.3063	1.563	0.675	9.38
ZZ PsA	0.078	0.1607	0.2984	1.993	0.575	4.03
SX Crv	0.079	0.1745	0.3241	1.624	0.733	8.16
V53	0.079	0.1703	0.3163	1.867	0.883	5.00
CRTS J224827.6 + 341351	0.079	0.1727	0.3208	1.726	0.686	6.61
AW UMa	0.080	0.1707	0.3172	2.097	1.133	3.33
KIC 10007533	0.081	0.1626	0.3021	2.145	1.538	3.05
CRTS J155009.2 + 493639	0.082	0.1694	0.3147	2.021	0.964	3.79
V870 Ara	0.082	0.1673	0.3108	1.885	0.911	4.82
KIC 8145477	0.082	0.1585	0.2944	2.076	1.370	3.42
CRTS J234634.7 + 222824	0.086	0.1569	0.2914	1.652	0.619	7.68
TYC 835-1081-1	0.086	0.1540	0.2860	1.961	0.855	4.20
CRTS J154254.0 + 324652	0.087	0.1557	0.2893	1.806	0.749	5.60
KIC 11144556	0.087	0.1518	0.2820	2.136	1.521	3.08
KIC 10596883	0.088	0.1435	0.2666	1.957	1.167	4.18
CRTS J155106.5 + 303534	0.089	0.1525	0.2833	1.862	0.799	5.02
1SWASP J132829.37+555246.1	0.089	0.1480	0.2750	1.844	0.647	5.22
ASAS J103737-3709.5	0.090	0.1456	0.2705	1.641	0.666	7.82
KIC 8804824	0.091	0.1375	0.2554	1.859	1.167	4.97
KIC 5374883	0.092	0.1465	0.2721	1.752	0.998	6.13
KR Com	0.093	0.1543	0.2867	1.778	0.309	6.01
CRTS J170307.9 + 020101	0.093	0.1420	0.2638	1.694	0.600	7.02
CRTS J223837.9 + 321932	0.093	0.1440	0.2676	1.991	0.920	3.96
KIC 7698650	0.095	0.1365	0.2537	2.042	1.444	3.57
CRTS J164000.2 + 491335	0.095	0.1402	0.2604	1.884	0.814	4.80
ASAS J153433+1225.3	0.096	0.1344	0.2497	1.722	0.938	6.50
CSS J233332.9+180430	0.096	0.1326	0.2463	2.128	1.382	3.10
FP Boo	0.096	0.1325	0.2461	2.085	0.965	3.38
KIC 11097678	0.097	0.2905	0.5396	2.439	0.204	1.99
CRTS J162327.1 + 031900	0.097	0.1384	0.2571	2.063	0.971	3.50
CRTS J133031.1 + 161202	0.098	0.1331	0.2472	1.684	0.634	7.13
KIC 9453192	0.099	0.1283	0.2384	2.183	1.657	2.83
NSVS 4701980	0.099	0.1331	0.2473	1.788	0.960	5.70
CRTS J160755.2 + 332342	0.099	0.1329	0.2470	1.811	0.745	5.50

Continuation of Table 13

Star	q	$J_{spin}/J_{orb}^*$	$J_{spin}/J_{orb}$	$M_{2i}$	$M_{1i}$	Age
NW Aps	0.100	0.0919	0.1707	2.205	0.706	2.82
AW CrB	0.101	0.1301	0.2417	1.965	0.777	4.15
DN Boo	0.103	0.1256	0.2334	1.902	0.839	4.62
ASAS J082243+1927.0	0.106	0.1193	0.2216	1.550	0.636	9.16
V1191 Cyg	0.107	0.1212	0.2252	1.831	0.742	5.28
CK Boo	0.109	0.1146	0.2128	1.794	0.881	5.60
NSVS 10368868	0.110	0.1162	0.2158	1.701	0.869	6.75
TYC 6995-813-1	0.111	0.1162	0.2159	2.013	0.599	3.83
ATO J022.8782+55.2989	0.111	0.1074	0.1995	1.770	0.776	5.89
FG Hya	0.112	0.1170	0.2173	1.759	0.913	5.98
CSS J110658.4+511201	0.119	0.1119	0.2079	1.933	0.971	4.31
ASASSN-V J022733.60+360447.1	0.120	0.1052	0.1953	1.935	0.994	4.28
V2787 Ori	0.120	0.1001	0.1860	1.970	0.835	4.06
V0566 Cam	0.121	0.0997	0.1852	1.984	1.031	3.92
GR Vir	0.122	0.1068	0.1983	1.824	0.814	5.27
NSVS 6798913	0.128	0.0980	0.1820	1.795	0.941	5.50
NSVS 7480723	0.128	0.0972	0.1806	1.621	0.896	7.82
eps CrA	0.128	0.0941	0.1748	2.060	1.085	3.42
ASAS J102556+2049.3	0.131	0.0916	0.1702	1.601	0.619	8.36
ASAS0154+20	0.137	0.0868	0.1612	1.870	1.376	4.64
V584 Cam	0.137	0.0912	0.1694	1.762	1.025	5.79
V776 Cas	0.138	0.0967	0.1797	2.047	1.079	3.49
V345 Gem	0.142	0.0904	0.1679	1.742	0.525	6.22
NSVS 3650324	0.142	0.0932	0.1732	1.980	0.895	3.93
V410 Aur	0.143	0.0861	0.1600	1.745	0.777	6.05
V710 Mon	0.143	0.0896	0.1664	1.924	0.547	4.42
DZ Psc	0.145	0.0918	0.1706	1.820	0.802	5.27
TIC 89428764	0.147	0.0815	0.1514	1.950	0.919	4.12
XY LMi	0.148	0.0854	0.1586	1.909	0.599	4.49
EM Psc	0.149	0.0883	0.1641	1.569	0.575	8.88
NX Cam	0.150	0.0723	0.1343	1.942	1.186	4.10
NSVS 5029961	0.151	0.0774	0.1438	1.795	1.364	5.26
TIC 321576458	0.153	0.0847	0.1573	1.917	0.617	4.43
MW Pav	0.154	0.0767	0.1425	2.523	0.909	1.76
NSVS 2643686	0.158	0.0854	0.1587	1.832	0.763	5.10
HV Aqr	0.159	0.0782	0.1453	1.777	0.507	5.78
V728 Her	0.160	0.0801	0.1487	2.083	1.194	3.24
CRTS J163819.6+03485	0.160	0.0792	0.1471	1.645	0.701	7.40
NSVS 1926064	0.160	0.0788	0.1463	1.852	1.019	4.82
V144	0.160	0.0729	0.1354	2.290	0.611	2.43
NSVS 2256852	0.161	0.0717	0.1332	1.603	0.462	8.27
TIC 393943031	0.163	0.0741	0.1377	1.950	0.822	4.10
AH Aur	0.165	0.0786	0.1459	2.038	1.084	3.47
TV Mus	0.166	0.0841	0.1562	1.923	0.778	4.31
AH Cnc	0.168	0.0734	0.1363	1.512	0.656	9.83
NSVS 13602901	0.171	0.0705	0.1310	1.861	0.633	4.85
AS CrB	0.172	0.0716	0.1330	1.938	0.669	4.22
CU Tau	0.177	0.0685	0.1273	1.569	0.743	8.58

Continuation of Table 13

Star	q	$J_{spin}/J_{orb}^*$	$J_{spin}/J_{orb}$	$M_{2i}$	$M_{1i}$	Age
V458 Mon	0.183	0.0636	0.1182	1.805	0.667	5.33
TY Pup	0.184	0.0718	0.1334	2.607	0.876	1.57
GV Leo	0.188	0.0635	0.1180	1.457	0.584	11.17
BO Ari	0.190	0.0584	0.1085	1.622	0.513	7.75
EK Aqr	0.192	0.0614	0.1140	2.266	1.150	2.41
Y Sex	0.195	0.0623	0.1158	1.910	1.020	4.25
CSS J022914.4+044340	0.198	0.0623	0.1157	1.633	0.989	7.14
V402 Aur	0.201	0.0223	0.0413	2.136	1.030	2.94
V1363 Ori	0.205	0.0592	0.1100	1.752	0.674	5.81
DN Aur	0.205	0.0588	0.1093	1.756	0.949	5.61
HI Pup	0.206	0.0554	0.1028	1.907	0.656	4.41
V429 Cam	0.208	0.0576	0.1070	1.936	0.804	4.11
TIC 159102550	0.211	0.0540	0.1003	1.886	0.865	4.45
NS Cam	0.213	0.0544	0.1010	2.134	0.547	3.02
V409 Hya	0.216	0.0573	0.1064	1.615	1.068	7.23
V830 Cep	0.228	0.0512	0.0950	1.621	0.359	7.77
YY Crb	0.232	0.0503	0.0935	1.822	0.895	4.88
KN Per	0.236	0.0515	0.0956	2.607	1.283	1.51
GSC 3208-1986	0.237	0.0502	0.0932	1.493	1.053	9.26
V921 Her	0.244	0.0474	0.0881	2.609	1.361	1.49
V1068 Her	0.266	0.0423	0.0786	1.805	0.537	5.17

\*Revised value

## REFERENCES

- Akerlof, C., Amrose, S., Balsano, R., et al. 2000, AJ, 119, 1901, doi: [10.1086/301321](https://doi.org/10.1086/301321)
- Alvarez, G. E., Sowell, J. R., Williamon, R. M., & Lapasset, E. 2015, Publications of the Astronomical Society of the Pacific, 127, 742, doi: [10.1086/682388](https://doi.org/10.1086/682388)
- Binnendijk, L. 1970, Vistas in Astronomy, 12, 217, doi: [https://doi.org/10.1016/0083-6656\(70\)90041-3](https://doi.org/10.1016/0083-6656(70)90041-3)
- Bob, N. 2011, Bob Nelson's database of eclipsing binary O-C files, <https://www.aavso.org/bob-nelsons-o-c-files>
- Brat, L., Trnka, J., Lehky, M., et al. 2009, Open European Journal on Variable Stars, 107, 1
- Brat, L., Trnka, J., Smelcer, L., et al. 2011, Open European Journal on Variable Stars, 137, 1
- Broens, E. 2013, MNRAS, 430, 3070, doi: [10.1093/mnras/stt113](https://doi.org/10.1093/mnras/stt113)
- Carroll, B. W., & Ostlie, D. A. 2017, An Introduction to Modern Astrophysics, 2nd edn., ed. S. F. P. Addison-Wesley
- Caton, D., Gentry, D. R., Samec, R. G., et al. 2019, Publications of the Astronomical Society of the Pacific, 131, 054203, doi: [10.1088/1538-3873/aafb8f](https://doi.org/10.1088/1538-3873/aafb8f)
- Chang, L., Zhu, L., & Meng, F. 2023, Research in Astronomy and Astrophysics, 23, 045017, doi: [10.1088/1674-4527/acc2a0](https://doi.org/10.1088/1674-4527/acc2a0)
- Counselman, Charles C., I. 1973, Astrophysical Journal, 180, 307, doi: [10.1086/151964](https://doi.org/10.1086/151964)
- Cox, A. N. 2000, Allen's astrophysical quantities
- Şenavcı, H. V., Doğruel, M. B., Nelson, R. H., Yılmaz, M., & Selam, S. O. 2016, PASA, 33, e043, doi: [10.1017/pasa.2016.39](https://doi.org/10.1017/pasa.2016.39)
- Şenavcı, H. V., Nelson, R. H., Özavcı, İ., Selam, S. O., & Albayrak, B. 2008, NewA, 13, 468, doi: [10.1016/j.newast.2008.01.001](https://doi.org/10.1016/j.newast.2008.01.001)
- Cui, X.-Q., Zhao, Y.-H., Chu, Y.-Q., et al. 2012, Research in Astronomy and Astrophysics, 12, 1197, doi: [10.1088/1674-4527/12/9/003](https://doi.org/10.1088/1674-4527/12/9/003)
- Deb, S., & Singh, H. P. 2011, Monthly Notices of the Royal Astronomical Society, 412, 1787, doi: [10.1111/j.1365-2966.2010.18016.x](https://doi.org/10.1111/j.1365-2966.2010.18016.x)
- Diethelm, R. 2001, Information Bulletin on Variable Stars, 5060, 1
- Drake, A. J., Graham, M. J., Djorgovski, S. G., et al. 2014, ApJS, 213, 9, doi: [10.1088/0067-0049/213/1/9](https://doi.org/10.1088/0067-0049/213/1/9)
- Eggen, O. J. 1967, MmRAS, 70, 111

- . 1968, Information Bulletin on Variable Stars, 308, 1  
 Er-gang, Z., Sheng-bang, Q., Soonthornthum, B., et al.  
 2019, ApJL, 871, L10, doi: [10.3847/2041-8213/aafc2e](https://doi.org/10.3847/2041-8213/aafc2e)
- Erkan, N., & Ulaş, B. 2016, NewA, 46, 73,  
 doi: [10.1016/j.newast.2015.12.009](https://doi.org/10.1016/j.newast.2015.12.009)
- Esa, . 1997, VizieR Online Data Catalog, I/239
- Ferreira, T., Saito, R. K., Minniti, D., et al. 2019, Monthly Notices of the Royal Astronomical Society, 486, 1220,  
 doi: [10.1093/mnras/stz878](https://doi.org/10.1093/mnras/stz878)
- Flannery, B. P. 1976, ApJ, 205, 217, doi: [10.1086/154266](https://doi.org/10.1086/154266)
- Gao, X.-Y., Cai, Y.-W., Li, K., Gao, A., & Shao, Y.-D.  
 2022, New Astronomy, 95, 101800,  
 doi: <https://doi.org/10.1016/j.newast.2022.101800>
- Gao, X.-Y., Cai, Y.-W., Li, K., Gao, A., & Shao, Y.-D.  
 2022a, NewA, 95, 101800,  
 doi: [10.1016/j.newast.2022.101800](https://doi.org/10.1016/j.newast.2022.101800)
- Gao, X.-Y., Li, K., Cai, Y.-W., et al. 2022b, PASP, 134,  
 114202, doi: [10.1088/1538-3873/ac99fd](https://doi.org/10.1088/1538-3873/ac99fd)
- Gazeas, K., Zola, S., Liakos, A., et al. 2021, MNRAS, 501,  
 2897, doi: [10.1093/mnras/staa3753](https://doi.org/10.1093/mnras/staa3753)
- Gazeas, K. D., Niarchos, P. G., Zola, S., Kreiner, J. M., &  
 Rucinski, S. M. 2006, AcA, 56, 127.  
<https://arxiv.org/abs/0903.1364>
- Gazeas, K. D., Baran, A., Niarchos, P., et al. 2005, AcA,  
 55, 123
- Godfrey, S. N., Leung, K. C., & Schmidt, E. G. 1996,  
 Astrophysics and Space Science, 246, 291,  
 doi: [10.1007/BF00645645](https://doi.org/10.1007/BF00645645)
- . 1997, Astrophysics and Space Science, 254, 295,  
 doi: [10.1023/A:1000874329854](https://doi.org/10.1023/A:1000874329854)
- Guo, D.-F., Li, K., Liu, F., et al. 2022, Monthly Notices of  
 the Royal Astronomical Society, 517, 1928,  
 doi: [10.1093/mnras/stac2811](https://doi.org/10.1093/mnras/stac2811)
- Gürol, B., Gürsoytrak, S. H., & Bradstreet, D. H. 2015,  
 NewA, 39, 9, doi: [10.1016/j.newast.2015.02.003](https://doi.org/10.1016/j.newast.2015.02.003)
- Hoňková, K., Juryšek, J., Lehký, M., et al. 2013, Open  
 European Journal on Variable Stars, 160, 1
- Hubscher, J. 2017, Information Bulletin on Variable Stars,  
 6196, 1, doi: [10.22444/IBVS.6196](https://doi.org/10.22444/IBVS.6196)
- Hubscher, J., Lehmann, P. B., Monninger, G., Steinbach,  
 H.-M., & Walter, F. 2010, Information Bulletin on  
 Variable Stars, 5918, 1
- Hubscher, J., Lehmann, P. B., & Walter, F. 2012,  
 Information Bulletin on Variable Stars, 6010, 1
- Hut, P. 1980, Astronomy and Astrophysics, 92, 167
- Kandulapati, S., Devarapalli, S. P., & Pasagada, V. R.  
 2015, MNRAS, 446, 510, doi: [10.1093/mnras/stu2000](https://doi.org/10.1093/mnras/stu2000)
- Kjurkchieva, D. P., Popov, V. A., & Petrov, N. I. 2018a,  
 Research in Astronomy and Astrophysics, 18, 129,  
 doi: [10.1088/1674-4527/18/10/129](https://doi.org/10.1088/1674-4527/18/10/129)
- . 2018b, AJ, 156, 77, doi: [10.3847/1538-3881/aace5e](https://doi.org/10.3847/1538-3881/aace5e)
- . 2020, NewA, 77, 101352,  
 doi: [10.1016/j.newast.2019.101352](https://doi.org/10.1016/j.newast.2019.101352)
- Kjurkchieva, D. P., Popov, V. A., Vasileva, D. L., & Petrov,  
 N. I. 2018c, NewA, 62, 46,  
 doi: [10.1016/j.newast.2018.01.008](https://doi.org/10.1016/j.newast.2018.01.008)
- Kopal, Z. 1956, Annales d'Astrophysique, 19, 298
- Kriwattanawong, W., & Poojon, P. 2013, Research in  
 Astronomy and Astrophysics, 13, 1330,  
 doi: [10.1088/1674-4527/13/11/004](https://doi.org/10.1088/1674-4527/13/11/004)
- Kwee, K. K., & van Woerden, H. 1956, Bulletin of the  
 Astronomical Institute of Netherlands, 12, 327
- Lapasset, E. 1974, Information Bulletin on Variable Stars,  
 917, 1
- . 1977, Ap&SS, 46, 155, doi: [10.1007/BF00643760](https://doi.org/10.1007/BF00643760)
- Li, F. X., Liao, W. P., Qian, S. B., et al. 2022a, ApJ, 924,  
 30, doi: [10.3847/1538-4357/ac3425](https://doi.org/10.3847/1538-4357/ac3425)
- Li, F.-X., Qian, S.-B., Fernández Lajús, E., Liu, L., & Zhao,  
 E.-G. 2022b, PASJ, 74, 533, doi: [10.1093/pasj/psac016](https://doi.org/10.1093/pasj/psac016)
- Li, K., Gao, X., Liu, X.-Y., et al. 2022, The Astronomical  
 Journal, 164, 202, doi: [10.3847/1538-3881/ac8ff2](https://doi.org/10.3847/1538-3881/ac8ff2)
- Li, K., Hu, S., Chen, X., & Guo, D. 2017, PASJ, 69, 79,  
 doi: [10.1093/pasj/psx064](https://doi.org/10.1093/pasj/psx064)
- Li, K., & Qian, S. B. 2013, NewA, 22, 57,  
 doi: [10.1016/j.newast.2013.01.006](https://doi.org/10.1016/j.newast.2013.01.006)
- Li, K., Xia, Q.-Q., Kim, C.-H., et al. 2021a, ApJ, 922, 122,  
 doi: [10.3847/1538-4357/ac242f](https://doi.org/10.3847/1538-4357/ac242f)
- . 2021b, AJ, 162, 13, doi: [10.3847/1538-3881/abfc53](https://doi.org/10.3847/1538-3881/abfc53)
- Li, L., & Zhang, F. 2006, MNRAS, 369, 2001,  
 doi: [10.1111/j.1365-2966.2006.10462.x](https://doi.org/10.1111/j.1365-2966.2006.10462.x)
- Li, X.-Z., Liu, L., & Zhu, L.-Y. 2020, PASJ, 72, 103,  
 doi: [10.1093/pasj/psaa104](https://doi.org/10.1093/pasj/psaa104)
- Liu, L., & Li, X.-Z. 2021, Research in Astronomy and  
 Astrophysics, 21, 180, doi: [10.1088/1674-4527/21/7/180](https://doi.org/10.1088/1674-4527/21/7/180)
- Liu, L., Chen, W. P., Na, W. W., et al. 2014, NewA, 31, 60,  
 doi: [10.1016/j.newast.2014.03.001](https://doi.org/10.1016/j.newast.2014.03.001)
- Liu, X.-Y., Li, K., Michel, R., et al. 2023, MNRAS, 519,  
 5760, doi: [10.1093/mnras/stad026](https://doi.org/10.1093/mnras/stad026)
- Lucy, L. B. 1967, Zeitschrift für Astrophysik, 65, 89
- . 1968, The Astrophysical Journal, 151, 1123,  
 doi: [10.1086/149510](https://doi.org/10.1086/149510)
- . 1976, ApJ, 205, 208, doi: [10.1086/154265](https://doi.org/10.1086/154265)
- Martignoni, M., Acerbi, F., & Barani, C. 2021, NewA, 84,  
 101512, doi: [10.1016/j.newast.2020.101512](https://doi.org/10.1016/j.newast.2020.101512)
- Michel, R., & Kjurkchieva, D. 2019, NewA, 68, 51,  
 doi: [10.1016/j.newast.2018.10.006](https://doi.org/10.1016/j.newast.2018.10.006)
- Na, W. W., Qian, S. B., Zhang, L., et al. 2014, NewA, 30,  
 105, doi: [10.1016/j.newast.2014.01.009](https://doi.org/10.1016/j.newast.2014.01.009)
- O'Connell, D. 1951, PRCO, 2, 85
- Pagel, L. 2020, BAV Journal, 033, 1

- Papageorgiou, A., Christopoulou, P.-E., Lalounta, E., et al. 2023, ApJ, 952, 141, doi: [10.3847/1538-4357/acdef3](https://doi.org/10.3847/1538-4357/acdef3)
- Pojmanski, G. 2002, AcA, 52, 397, doi: [10.48550/arXiv.astro-ph/0210283](https://doi.org/10.48550/arXiv.astro-ph/0210283)
- Popov, V. A., & Petrov, N. I. 2022, NewA, 97, 101862, doi: [10.1016/j.newast.2022.101862](https://doi.org/10.1016/j.newast.2022.101862)
- Pribulla, T., Kreiner, J. M., & Tremko, J. 2003, Contributions of the Astronomical Observatory Skalnate Pleso, 33, 38
- Qian, S. 2001, Monthly Notices of the Royal Astronomical Society, 328, 914, doi: [10.1046/j.1365-8711.2001.04921.x](https://doi.org/10.1046/j.1365-8711.2001.04921.x)
- Qian, S. 2003, Monthly Notices of the Royal Astronomical Society, 342, 1260, doi: [10.1046/j.1365-8711.2003.06627.x](https://doi.org/10.1046/j.1365-8711.2003.06627.x)
- Qian, S., & Yang, Y. 2005, Monthly Notices of the Royal Astronomical Society, 356, 765, doi: [10.1111/j.1365-2966.2004.08497.x](https://doi.org/10.1111/j.1365-2966.2004.08497.x)
- Qian, S. B., He, J. J., Soonthornthum, B., et al. 2008, AJ, 136, 1940, doi: [10.1088/0004-6256/136/5/1940](https://doi.org/10.1088/0004-6256/136/5/1940)
- Qian, S.-B., He, J.-J., Zhang, J., et al. 2017, Research in Astronomy and Astrophysics, 17, 087, doi: [10.1088/1674-4527/17/8/87](https://doi.org/10.1088/1674-4527/17/8/87)
- Qian, S. B., Li, K., Liao, W. P., et al. 2013, AJ, 145, 91, doi: [10.1088/0004-6256/145/4/91](https://doi.org/10.1088/0004-6256/145/4/91)
- Qian, S.-B., Liu, L., Soonthornthum, B., Zhu, L.-Y., & He, J.-J. 2006, The Astronomical Journal, 131, 3028, doi: [10.1086/503561](https://doi.org/10.1086/503561)
- Qian, S. B., Liu, L., Zhu, L. Y., et al. 2011, AJ, 141, 151, doi: [10.1088/0004-6256/141/5/151](https://doi.org/10.1088/0004-6256/141/5/151)
- Qian, S. B., & Yang, Y. G. 2004, The Astronomical Journal, 128, 2430, doi: [10.1086/425051](https://doi.org/10.1086/425051)
- Qian, S. B., Yang, Y. G., Soonthornthum, B., et al. 2005a, The Astronomical Journal, 130, 224, doi: [10.1086/430673](https://doi.org/10.1086/430673)
- Qian, S. B., Zhang, J., He, J. J., et al. 2018, The Astrophysical Journal Supplement Series, 235, 5, doi: [10.3847/1538-4365/aaa601](https://doi.org/10.3847/1538-4365/aaa601)
- Qian, S.-B., Zhu, L.-Y., Liu, L., et al. 2020, Research in Astronomy and Astrophysics, 20, 163, doi: [10.1088/1674-4527/20/10/163](https://doi.org/10.1088/1674-4527/20/10/163)
- Qian, S. B., Zhu, L. Y., Soonthornthum, B., et al. 2005b, The Astronomical Journal, 130, 1206, doi: [10.1086/432544](https://doi.org/10.1086/432544)
- Rahunen, T. 1981, Astronomy and Astrophysics, 102, 81
- Richards, T., Blackford, M., Bohlsen, T., et al. 2017, Open European Journal on Variable Stars, 182, 1
- Richards, T., Blackford, M., Butterworth, N., Evans, P., & Jenkins, R. 2016, Open European Journal on Variable Stars, 177, 1
- Ricker, G., Winn, J., Vanderspek, R., et al. 2014, Journal of Astronomical Telescopes, Instruments, and Systems, 1, doi: [10.1111/JATIS.1.1.014003](https://doi.org/10.1111/JATIS.1.1.014003)
- Robertson, J. A., & Eggleton, P. P. 1977, MNRAS, 179, 359, doi: [10.1093/mnras/179.3.359](https://doi.org/10.1093/mnras/179.3.359)
- Ruciński, S. M. 1969, AcA, 19, 245
- Ruciński, S. M. 2007, MNRAS, 382, 393, doi: [10.1111/j.1365-2966.2007.12377.x](https://doi.org/10.1111/j.1365-2966.2007.12377.x)
- Ruciński, S. M., & Duerbeck, H. W. 2006, AJ, 132, 1539, doi: [10.1086/507025](https://doi.org/10.1086/507025)
- Samec, R. G., Chamberlain, H., Caton, D., et al. 2020, JAAVSO, 48, 150
- Samec, R. G., Kring, J. D., Robb, R., Van Hamme, W., & Faulkner, D. R. 2015, AJ, 149, 90, doi: [10.1088/0004-6256/149/3/90](https://doi.org/10.1088/0004-6256/149/3/90)
- Sarotsakulchai, T., Qian, S. B., Soonthornthum, B., et al. 2018, AJ, 156, 199, doi: [10.3847/1538-3881/aadcf](https://doi.org/10.3847/1538-3881/aadcf)
- Selam, S. O. 2004, A&A, 416, 1097, doi: [10.1051/0004-6361:20034578](https://doi.org/10.1051/0004-6361:20034578)
- Singh, M., & Chaubey, U. S. 1986, Ap&SS, 124, 389, doi: [10.1007/BF00656049](https://doi.org/10.1007/BF00656049)
- Sriram, K., Malu, S., Choi, C. S., & Vivekananda Rao, P. 2016, The Astronomical Journal, 151, 69, doi: [10.3847/0004-6256/151/3/69](https://doi.org/10.3847/0004-6256/151/3/69)
- Szalai, T., Kiss, L. L., Mészáros, S., Vinkó, J., & Csizmadia, S. 2007, A&A, 465, 943, doi: [10.1051/0004-6361:20066768](https://doi.org/10.1051/0004-6361:20066768)
- Tang, Y.-K., Guo, Y.-N., Li, K., Gai, N., & Li, Z.-K. 2022, Research in Astronomy and Astrophysics, 22, 035009, doi: [10.1088/1674-4527/ac4705](https://doi.org/10.1088/1674-4527/ac4705)
- Tian, X.-m., Zhu, L.-y., & Wang, Z.-h. 2019, PASP, 131, 084203, doi: [10.1088/1538-3873/ab221e](https://doi.org/10.1088/1538-3873/ab221e)
- Tody, D. 1986, in Instrumentation in Astronomy VI, ed. D. L. Crawford, Vol. 0627, International Society for Optics and Photonics (SPIE), 733 – 748, doi: [10.1117/12.968154](https://doi.org/10.1117/12.968154)
- Tody, D. 1993, in Astronomical Society of the Pacific Conference Series, Vol. 52, Astronomical Data Analysis Software and Systems II, ed. R. J. Hanisch, R. J. V. Brissenden, & J. Barnes, 173
- Tran, K., Levine, A., Rappaport, S., et al. 2013, ApJ, 774, 81, doi: [10.1088/0004-637X/774/1/81](https://doi.org/10.1088/0004-637X/774/1/81)
- Ulaş, B., Kalomeni, B., Keskin, V., Köse, O., & Yakut, K. 2012, NewA, 17, 46, doi: [10.1016/j.newast.2011.06.002](https://doi.org/10.1016/j.newast.2011.06.002)
- Ulaş, B., & Ulusoy, C. 2014, NewA, 31, 56, doi: [10.1016/j.newast.2014.02.009](https://doi.org/10.1016/j.newast.2014.02.009)
- van Hamme, W. 1993, AJ, 106, 2096, doi: [10.1086/116788](https://doi.org/10.1086/116788)
- Wadhwa, S. S. 2005, Astrophysics and Space Science, 300, 329.  
<https://api.semanticscholar.org/CorpusID:120884731>
- Wadhwa, S. S., Arbutina, B., Petrović, J., et al. 2023, PASP, 135, 094201, doi: [10.1088/1538-3873/acf40d](https://doi.org/10.1088/1538-3873/acf40d)

- Wadhwa, S. S., de Horta, A. Y., Filipović, M. D., & Totohill, F. H. N. 2022, Journal of Astrophysics and Astronomy, 43, 42, doi: [10.1007/s12036-022-09832-9](https://doi.org/10.1007/s12036-022-09832-9)
- Wadhwa, S. S., De Horta, A., Filipović, M. D., et al. 2020, Monthly Notices of the Royal Astronomical Society, 501, 229, doi: [10.1093/mnras/staa3637](https://doi.org/10.1093/mnras/staa3637)
- Wadhwa, S. S., Tothill, N. F. H., DeHorta, A. Y., & Filipović, M. 2021, Research in Astronomy and Astrophysics, 21, 235, doi: [10.1088/1674-4527/21/9/235](https://doi.org/10.1088/1674-4527/21/9/235)
- Williamon, R. M. 1971, Information Bulletin on Variable Stars, 574, 1
- Wilson, R. E., & Devinney, E. J. 1971, ApJ, 166, 605, doi: [10.1086/150986](https://doi.org/10.1086/150986)
- Wilson, R. E., & Van Hamme, W. 2014, ApJ, 780, 151, doi: [10.1088/0004-637X/780/2/151](https://doi.org/10.1088/0004-637X/780/2/151)
- Wu, Y., Singh, H. P., Prugniel, P., Gupta, R., & Koleva, M. 2011, A&A, 525, A71, doi: [10.1051/0004-6361/201015014](https://doi.org/10.1051/0004-6361/201015014)
- Yang, Y. 2008, Ap&SS, 314, 151, doi: [10.1007/s10509-008-9751-5](https://doi.org/10.1007/s10509-008-9751-5)
- Yang, Y., Wang, S., Yuan, H., & Dai, H.-G. 2021, Research in Astronomy and Astrophysics, 21, <https://api.semanticscholar.org/CorpusID:244474365>
- Yang, Y.-G., & Qian, S.-B. 2015, AJ, 150, 69, doi: [10.1088/0004-6256/150/3/69](https://doi.org/10.1088/0004-6256/150/3/69)
- Yang, Y.-G., Qian, S.-B., & Soonthornthum, B. 2012, The Astronomical Journal, 143, 122, doi: [10.1088/0004-6256/143/5/122](https://doi.org/10.1088/0004-6256/143/5/122)
- Yang, Y. G., Qian, S. B., & Zhu, L. Y. 2005a, AJ, 130, 2252, doi: [10.1086/496880](https://doi.org/10.1086/496880)
- Yang, Y. G., Qian, S. B., Zhu, L. Y., & He, J. J. 2009, AJ, 138, 540, doi: [10.1088/0004-6256/138/2/540](https://doi.org/10.1088/0004-6256/138/2/540)
- Yang, Y.-G., Qian, S.-B., Zhu, L.-Y., He, J.-J., & Yuan, J.-Z. 2005b, PASJ, 57, 983, doi: [10.1093/pasj/57.6.983](https://doi.org/10.1093/pasj/57.6.983)
- Yıldız, M. 2014, MNRAS, 437, 185, doi: [10.1093/mnras/stt1874](https://doi.org/10.1093/mnras/stt1874)
- Yıldız, M., & Doğan, T. 2013, Monthly Notices of Royal Astronomical Society, 430, 2029, doi: [10.1093/mnras/stt028](https://doi.org/10.1093/mnras/stt028)
- Yin, Z.-X., Meng, Z.-B., Wu, P.-R., et al. 2023, Research in Astronomy and Astrophysics, 23, 085013, doi: [10.1088/1674-4527/acd73c](https://doi.org/10.1088/1674-4527/acd73c)
- Zhang, X. B., Z. R. X., & Deng, L. 2005, The Astronomical Journal, 129, 979, doi: [10.1086/426914](https://doi.org/10.1086/426914)
- Zhao, E. G., Qian, S. B., Zhou, X., et al. 2021, MNRAS, 504, 5155, doi: [10.1093/mnras/stab1188](https://doi.org/10.1093/mnras/stab1188)
- Zhao, E.-g., & Tian, X.-m. 2022, NewA, 94, 101778, doi: [10.1016/j.newast.2022.101778](https://doi.org/10.1016/j.newast.2022.101778)
- Zheng, S.-Y., Li, K., & Xia, Q.-Q. 2021, MNRAS, 506, 4251, doi: [10.1093/mnras/stab1829](https://doi.org/10.1093/mnras/stab1829)
- Zhou, X., Soonthornthum, B., Qian, S. B., & Fernández Lajús, E. 2019, MNRAS, 489, 4760, doi: [10.1093/mnras/stz2508](https://doi.org/10.1093/mnras/stz2508)
- Zhu, L.-Y., Zhao, E.-G., & Zhou, X. 2016, Research in Astronomy and Astrophysics, 16, 68, doi: [10.1088/1674-4527/16/4/068](https://doi.org/10.1088/1674-4527/16/4/068)
- Zhu, L. Y., Qian, S. B., Soonthornthum, B., et al. 2014, The Astronomical Journal, 147, 42, doi: [10.1088/0004-6256/147/2/42](https://doi.org/10.1088/0004-6256/147/2/42)
- Zola, S., Rucinski, S. M., Baran, A., et al. 2004, AcA, 54, 299
- Zubairi, A. W., Sheng-Bang, Q., gang Zhao, E., & Li, F.-X. 2023, Under review in ApJL
- Zubairi, A. W., Zhou, X., Fernández Lajús, E., et al. 2023, NewA, 100, 101989, doi: [10.1016/j.newast.2022.101989](https://doi.org/10.1016/j.newast.2022.101989)